WIND-TUNNEL MODELING OF THE FLOW ABOUT BLUFF BODIES

by

Robert N. Meroney*

Prepared for

Sonderforchungsbereich 210
"Stromungsmechanische Bemessungsgrundlagen
fur Bauwerke"

University of Karlsruhe
July 1986

*Professor-in-charge
Fluid Mechanics and Wind Engineering Program
Colorado State University

CEM86-87-RNM48

SUBJECT: WIND-TUNNEL MODELING OF THE FLOW ABOUT BLUFF BODIES

DATE: July, 1986

BY: Robert N. Meroney, Professor
Fluid Mechanics and Wind Engineering Program
Colorado State University

INTRODUCTION:

Wind flowing around bluff bodies and structures results in a distribution of pressures about the bodies. These pressures act over the surface to produce mean and local forces which may damage or uncomfortably vibrate the body or to produce local wind environments which may transport noxious gases or buffet pedestrians. This review will consider the state of understanding of flow around simple rectangularly-shaped bluff bodies resulting from wind-tunnel studies of mean surface-pressure patterns. Evidence for similarity is examined, and recommendations provided for future research.

BACKGROUND:

Engineers began to incorporate the influence of the wind in their designs during the nineteenth century. The Firth of Forth Bridge, Scotland, the Eifel tower, Paris, and the Empire State Building, New York, are well known structures engineered for wind effects. Wind tunnels were used to evaluate wind loads by even the earliest investigators. In 1891 Irminger studied wind pressures on a small model house (flat , saddle, and rounded roofs) as well as two-dimensional plates, prisms, and cylinders suspended in the exhaust of a smoke stack.

Bailey in 1933 and Irminger and Nokkentved in 1936 compared pressures measured over building models placed in uniform flow fields in wind tunnels with full scale measurements over small buildings. Data scatter was so large that the original paper was inconclusive. Davenport's (1982) reanalysis of Bailey's experiment shows that the field and uniform wind tunnel results are not in good agreement. Later Bailey and Vincenta in 1943 measured flow over a similar model in a deep boundary layer. Their measurements agree considerably better with the field data.

Pessimism over the disagreement between uniform flow wind tunnel measurements and field experience led many engineers away from wind tunnel experiments, but in the early 1950's several investigators returned to the boundary-layer wind tunnel. Jensen (1954, 1958, 1963) systematically examined the effect of different boundary layer shear profiles on flow over shelter belts, chimney plumes, walls, and houses. Their comparison of wind tunnel and field measurements showed that the parameter L/Z_o (L being characteristic model length, Z_o is the boundary-layer roughness length) had a profound effect on the flow and pressure distribution. Strom at New York University and Cermak at Colorado State University were also early proponents of the need for

deep turbulent boundary layers to simulate the atmospheric boundary layer.

UNIFORM FLOW MEASUREMENTS:

Despite the evidence of Bailey and Vincenta, Jensen and others that the boundary layer affected surface pressures profoundly, researchers continued to predict surface forces based on models immersed in uniform flow fields until the mid 1970's. Typically, pressure coefficients produced during uniform flow experiments were combined with estimates of full scale winds which varied with height. This approach assumes Eifel's model law is valid, which expressed mathematically is $f_1(Cp, \theta, \text{geometry}) = 0$. The designers argued this method was effective because:

a. Uniform flow field pressure coefficients seemed to exceed values found in shear flows; hence, they were conservative,

b. Too few reliable atmospheric boundary layer measurements existed to justify an attempt to model atmospheric characteristics, and

c. Modeling the surface layer was often inconvenient, required special facilities, and added unnecessary expense.

Exhaustive studies of the effects of uniform flow over bluff bodies is summarized in the work of Chien et al. (1951). This report provides an extensive collection of surface pressure patterns over simply-gabled block-type structures, thin walls, hanger-type structures, and building clusters. They considered rectangular blocks with length to width (L/B) ratios varying from 0.25 to 4.00 and length to height (L/H) ratios varying from 0.13 to 1.5. For bodies whose front wall is placed normal to the wall they found minimum roof pressure coefficients, $Cp_H = p/(\rho U_H^2/2)$, of -1.00, but when the buildings were placed obliquely to the wind (45^o) the values were as low as -7.00.

Of course, considerable care had to be taken in the wind tunnel to arrive at consistent results. Since the earliest part of this century researchers have known that flow over sharp-edged bodies seemed to be insensitive to Reynolds number. Nonetheless, as measurement techniques improved up to 60% differences between investigators results were tiresomely apparent. Leutheusser and Baines (1967) reviewed the techniques used to suspend models in the potential flow core of wind tunnels. A model and its "mirror" image was often mounted on opposite sides of a common "ground" plate which extended in the downstream direction. The offset of the model from the ground plate front edge and length of the trailing distance of the ground plates were found to be most critical. Short ground plates did not seal the wake cavity of the models and permitted air to bleed into the cavity, consequently raising the base pressures.

Leutheusser and Baines also report that Reynolds numbers in excess of 2×10^5 were required to produce constant pressure coefficients. Scruton and Rogers (1971) report that rounding the corners of a square prism by a radius of B/6 or greater could lead to a Reynolds-number

dependency of drag coefficient similar to that found for a circular cylinder.

Three other parameters which can affect the pressure patterns on rectangular buildings in uniform flow are the turbulence intensity, u'/U, the longitudinal integral length, L_{ux}, and wind-tunnel blockage, A_m/A_{wt}. Hunt (1982) summarizes recent work on the effect of grid-generated turbulence structure on the flow around two dimensional bluff bodies. Various studies examined values of intensity from u'/U = 0.07 to 0.16, integral scales from L_{ux}/L = 0.7 to 5 and blockages, A_m/A_{wt} to 0.25. He concluded:

a. Turbulence acting along the separating streamline in the approach flow increases the separation shear flow thickness and entrainment, resulting in greater streamline curvature around the body. If the streamline does not reattach to the body, then base pressures are less and total base drag higher. If the body is long enough to permit streamline reattachment, then the vortex formation region moves downstream, thus raising the base pressure. Suction pressures inside the zone contained by the separating stream line will become stronger, since the strong streamline curvature requires lower pressures toward the center of curvature. Hence, local pressure coefficients may be up to 60% larger in turbulent uniform flow.

b. The effects of integral scale are less conclusive. Some authors claim to see up to a 40% change in base pressure with integral length, whereas other results indicated that for a sharp edged bluff body the effect of scale was small. If the integral scale becomes larger at the expense of energy contained in the scales of the size of the separating shear layer, then reattachment is less likely, base pressure drag remains large, and local pressure coefficients on the roof or sides small. If the integral length is of the same order of size as the small scale turbulence being entrained into the shear layers, then an increase in integral length will have only small effects.

c. Blockage effects on a two dimensional body can be considerable. If L_m/L_{wt} is 0.05 then Petty (1979) observed a 10% change in base pressure. Of course, three dimensional prisms of the same body width will block much less of the flow. Nonetheless, recent measurements made in various German wind tunnels and tabulated at the U. of Munich suggest that pressure coefficients vary significantly with blockage even for small values.

BOUNDARY-LAYER FLOW MEASUREMENTS:

According to the scaling law of Jensen (1958), the flow field and its effects on bluff bodies are modeled exactly if the bodies are geometrically similar in model and prototype, and if the dynamics of the flow field are such that H/Z_o are the same, where Z_o is the roughness height of the surface, and H is the height of the body. The model law implied by this statement is $f_2(Cp_H, \theta,$ geometry, $H/Z_o) = 0.0$.

Jensen and Franck suggested in principle that the velocity pressure at each measurement height should be used to calculate the pressure coefficient. In practice they felt that some arbitrary reference height or the velocity at roof height must be preferred. For the top of the body or roofs little difference is found between the two methods, but near the ground differences would be large. They also expressed a "physicist" distaste for coefficient values greater than 1. They also used friction velocity, u_*, as a reference velocity when considering concentrations; although, they do not propose it in their report for pressure coefficients.

Jensen and Franck (1958) examined pressure coefficients on small model houses for blockage effects. They concluded that when A_m/A_{wt} was less than 0.05 (5%) systematic errors would be less than 11% for windward roof pressures and even less in other locations. Jensen's model also implies independence of the Reynolds number; obviously, a minimum Reynolds number depending upon body shape is required even for sharp-edged bodies. Plate (1982) suggests a minimum value of 5×10^4.

For smooth surfaces, Z_o is about $0.11\nu/u_*$; hence, H/Z_o is equivalent to a shear Reynolds number, Hu_*/ν. Good and Joubert (1968) examined the drag of sharp edged fences placed along smooth walls. Ranga Raju et al. (1976) considered the drag of such fences placed along rough walls. They concluded similarity exists for the drag coefficient, $C_{D*} = F/(\rho u_*^2/2)$, when it is correlated against H/Z_o. Ranga Raju et al. suggest that "such a relation also exists for geometrically similarly shaped bluff bodies with sharp edges, provided their dimension in the flow direction is not large enough to cause reattachment of the boundary layer on the body itself." The model law implied by this statement is $f_3(Cp_{H*}, \theta, \text{geometry}, H/Z_o \text{ or } Hu_*/\nu) = 0.0$.

Sakamoto et al. (1982) measured pressure over small cubes placed within turbulent boundary layers growing over smooth surfaces. They found that the total drag for a cube correlated well as C_{D*} versus Hu_*/ν. Bachlin et al. (1982) considered roof-pressure coefficient behavior over rectangular blocks placed within turbulent boundary layers developing over rough surfaces. They concluded that maximum roof pressures for flows normal to a building face could be predicted by the empirical expression, $Cp_{max*} = 31.6\ (H/Z_o)^{0.29}$.

Unfortunately, any drag or pressure coefficient expression using the friction velocity, u_*, as the characteristic velocity and H/Z_o as the abscissa will be biased to produce strong correlations. Even a random number constrained to vary between say 0.5 and 1.0 will give the impression of strong correlation to a totally independent parameter when plotted in such a manner. This point is considered further in Appendix A; however, one must conclude that plots of C_{D*} or Cp_* versus H/Z_o or Hu_*/ν is inadvisable since the velocity scale used can itself explain more than 90% of the variance found in the resulting data plot.

Nonetheless, as recognized by Ranga Raju et al. (1976), Sakamoto et al. (1982), and Bachlin et al. (1982) the correlation suggested by

Jensen is not adequate when the height of the object becomes large with respect to boundary-layer thickness. Indeed, Leutheusser and Baines (1967) concluded from a re-examination of their own as well as Jensen and Franck's data that the actual model law must be expressed by $f_4(Cp_H, \theta, \text{geometry}, Re_H, Z_o/\delta$, and $\delta/H) = 0.0$. (Note, various combinations and products of these parameters are also possible, eg. Re_{Zo}, H/Z_o and H/δ .)

LOCAL PRESSURE COEFFICIENTS:

It is apparent that the boundary layer characteristics (such as u_*, Z_o, L_{xu}, δ , and u'/U) as well as depth of block immersion (H/δ^*) affect local pressure coefficient magnitudes and patterns. As noted by Peterka, Kothari and Meroney (1984) and Meroney (1982) the flow around a three dimensional block body is quite complex. The presence of the ground plate "horse shoe" vortex, separation at top and side wall corners, reattachment of streamlines to roof or side walls, and the orientation of the "delta wing" vortex on the roof strongly affect surface pressure patterns. None of these features are present for two-dimensional fences; although, reattachment may occur for a two-dimensional step.

For two dimensional steps the pressure distribution over the front face of the step could be predicted analytically by Meroney (1985) assuming only an inviscid rotational flow. This suggests the pressure distribution on a fence and consequently the fence drag are only dependent on the approach velocity distribution, and not particularly dependent on boundary layer turbulence. Examination of the data of Ranga Raju et al. (1976) and Good and Joubert (1968) suggests almost all variance in drag can be eliminated by using fence-height dynamic pressure as reference pressure, ie. $C_{Do} = F/(\rho\, U_H^2 H/2)$.

The surface pressures on the front surface of a rectangular body placed normal to the flow may also be expected to vary primarily with approach flow velocity distribution. The pressure distributions along the front centerline of a cube normalize remarkably well against the peak pressure located at a height of about $z/H = 0.75$ (Sakamoto et al., 1982, Fig. 3; Castro and Robins, 1977, Fig. 4(a); etc.) The data of Aikens (1976) for blocks of various face aspect ratios were plotted in terms of $Cp' = p(z,y)/(\rho\, U(z)^2/2)$. He found very little deviation in pattern shape until very slender bodies were examined. Corke and Nagib (1979) examined a square cross-section building in four different boundary layers. They collapsed the front face pressure coefficients with the expression $CCp = p(z,y)/[\rho\,\{U(z) + nu'(z)\}^2/2]$, where $n = 1.0$. The method eliminated all but 17% of the deviations caused by different boundary layers. The effects of roughness and boundary layer immersion on a front face pressure coefficient observed by Leutheusser (1965) and Leutheusser and Baines (1967) are also most likely explained by variations in approach wind speed at pressure tap height.

The effects of a shear velocity profile on the flow pattern around three-dimensional bodies was investigated by Baines (1963). On the front face of a building the effect of the shear profile is to move

the stagnation point up to about z/H = 0.75, and to form a cross stream vortex at the base of the wall. The shear profile (and associated turbulence) produces a much greater pressure recovery with a lower negative peak pressure at the front of the roof (-0.9 to -1.0 cf -0.6) recovering to a higher base or back wall pressure (-0.2 to -0.3 cf -0.6).

The work of Castro and Robins (1977), Dianant and Castro (1984), and Hosker (1984) suggest that reattachment of the separating stream line in a permanent or intermittent manner can have a major effect on roof, side and back surface pressure coefficients. The tendency to reattach increases as L/B increases. It is also very likely that the major influence of turbulence intensity and scale are on the behavior of the separating and reattaching streamlines about the body. Since turbulence intensity decreases with height, and longitudinal scale increases and then decreases with height, the roof and side pressure patterns must be affected by H/δ . Castro and Robins (1977) saw the flow switch from reattached to separated in the H/ range from 1.2 to 1.6 on a cube. Robins (1984) quotes unpublished data for a square-roofed model (L/δ = 1/8, H/δ = 1/8 to 3/4) where the critical range, in which flow switched from reattaching to fully separated, was from 1/2 to 3/4. He notes that for L/B < 1 the critical regime occurs at lower values of H/δ . Robins concludes that for rigorous modeling then f(Cp, θ, geometry, $u_*/U\infty$, Z_o/H, H/δ , u'/U, etc) = 0.0 is required.

For a block building normal to the approach wind the effect of separation or reattachment is to produce completely different flow fields. Dianat and Castro (1984) measured mean and fluctuating pressures and surface shear stress on the roof of several wide bodies of different streamwise lengths with their front faces placed normal to the approach wind. They found that with full separation the entire roof top tends to have nearly constant pressures, whereas, when the flow reattaches a pressure minimum occurs near the leading edge. Pressure and shear stress fluctuations are likely to be maximum during intermittent reattachment situations. It is very likely that the major influence of turbulence intensity and scale are on the behavior of the separating and reattaching streamlines about the body. One might logically expect that a fruitful correlation of roof surface pressures would be $f_6(Cp_H, \theta, \text{geometry}, (u'/U)_H) = 0.0$.

RE-EXAMINATION OF AVAILABLE Cp DATA:

Attached as Table 1 is a summary of available wind-tunnel experiments for flow over rectangular bodies for which the authors report local surface pressure measurements. Flow field conditions, model conditions, and maximum or minimum pressure coefficients on the roof, and front, side and back walls are tabulated as available. In some cases power law coefficient, roughness length, momentum thickness (Theta) or velocity at roof height are calculated from information provided by the authors. Figures 1 to 11 consider surface pressure coefficient behavior for blocks with their front face oriented normal to the wind. Figures 12 and 13 display limited data for a 45 degree orientation. Figures 14 and 15 consider the parameter space covered

by existing measurements.

Roof Pressures:

Figure 1 displays roof pressure coefficients, Cp_*, plotted versus H/Z_o ratio. This plot may be a better test of the reliability of the author's friction velocity and roughness length information than of the variation of roof pressures (See Appendix A). The data of Bachlin et al. (1982), Stathopoulos (1975, 1981, 1981), and Jensen and Franck (1958) seem to suggest a power law growth with H/Z_o and a coefficient near 0.3. The other data scatter widely; hence, their friction velocity values should be viewed with suspicion.

In Figures 2 through 11 the surface pressure coefficient, Cp_H, is defined in terms of the velocity at roof height. In Figure 2 roof pressures are generally found to decrease from -0.6 to -0.8 to -0.9 as the Delta/H ratio increases. A marked change seems to occur between Delta/H values of 0.75 and 1.5. This may be associated with the critical depth for reattachment of the separation stream line identified by Robins (1984). Some of the data of Arie et al. (1975) seems suspect, since it is unlikely that roof pressures decrease below -1.0 for a normal wind flow orientation.

Front-wall Pressures:

Figures 3, 4 and 5 for the front, side and back pressures display the very limited data available. The largest set of data was provided by Leutheusser (1965). It is surprising more information is not available for these regions. In Figure 3 the maximum front surface pressure coefficient decreases from 1.0 to 0.8 as Delta/H increases. Again a marked change occurs between Delta/H values of 0.75 and 1.5. This may represent a region of intermittent separation.

Side-wall and Back-wall Pressures:

Figure 4 displays side wall minimum pressure coefficients. Notice the transition to lower pressures at about Delta/H = 0.75. Since the radius of curvature of a reattached stream line is smaller than that of a separated streamline, pressures are generally lower inside the bound vortex. Pressure coefficients on the back wall of the body are shown in Figure 5. Base pressures increase at critical Delta/H values near 0.75 as the roof and side wall separation streamlines reattach to their own surfaces respectively.

Influence of Turbulence Intensity:

Figures 6 through 10 consider the influence of longitudinal turbulent intensity on surface pressure coefficients. Roof pressures are considered in both Figures 6 and 7. On Figure 6 turbulent intensities for the Bachlin et al. (1982) data are estimated with the formula, $u'/U_H = 1/\ln(H/Z_o)$. This formulae is often recommended for atmospheric flows, but it is usually found to overpredict turbulence values near the edge of the wind-tunnel boundary layer. Consequently, the relation $u'/U_H = \propto (1 - H/Delta)$ is used with the Bachlin et al.

data in Figure 7. Although scatter is large one can perceive a decrease in minimum roof pressure as intensities exceed 10%.

Front-wall pressure coefficients displayed on Figure 8 do not appear to correlate with turbulent intensity. This is not unexpected, since front wall surfaces do not involve separation stream lines.

Side-wall pressure coefficients on Figure 9 display the same trends as roof pressure coefficients.

On Figure 10 the data of Hunt (1982) suggest a decrease in base pressure as turbulent intensity increases. Although on first examination this behavior does not agree with the model suggested for the effects of separating streamline reattachment; nonetheless, all values are larger than -0.3 when turbulent intensity exceeds 10%. Recall from Figure 5 that for small values of Delta/H (ie. implies low values of u'/U) the base pressure coefficient was -0.6.

Surface Pressures on Obliquely Oriented Bodies:

Figures 11 and 12 display Cp_* versus H/Z_o and Cp_H versus Delta/H respectively for a rectangular body orientation of 45 degrees. Tentatively one may conclude from the very limited data that minimum roof pressure coefficients become less negative with body immersion in the boundary layer. Or one might argue that turbulence reduces the circulation intensity of the delta-wing roof vorticies.

Consistency Between Pressure Data:

Finally, for the zero degree wind orientation the various pressure coefficients are correlated against one another (Figure 13). The minimum roof pressure coefficient is used as the abscissa. Note that front-wall pressure coefficients seem uncorrelated with roof or side wall behavior. This supports the contention that front face pressures are not substantially influenced by the behavior of separating streamlines. Side-wall pressures seem to be linearly correlatable with roof pressures, and back-wall pressures correlate inversely with roof minimums. Again these variations agree with a model where the separation streamline vortex intensity and reattachment location govern roof, side-wall and back-wall pressures.

EXPERIMENTAL ENVELOPES:

As shown in summary Figure 14 most experiments to date have been performed within the envelope space of Length/Width ranging from 1 to 3 and Height/Length ranging from 0 to 3. Since greater slenderness ratios are typical for modern apartment buildings and skyscrapers, additional measurements for bodies with Height/Length ratios greater than 3 would be appropriate.

Figure 15 summarizes the range of boundary layer to bluff body scales examined in the wind tunnel. Field values for roughness length vary from 0.1 cm to 2 m, the atmospheric boundary depth may vary from 200 to 1000 m, and typical building heights vary from 3 m to 100 m. This

suggest a usable range of data should extend from $0 < \log(H/Z_o) < 5$ and $0.3 < \log(Delta/H) < 2.5$. There is very little data currently on block body behavior for $\log(Delta/H) > 1$. It would be valuable to examine bluff bodies in deep boundary flows of medium to large turbulent intensity and large longitudinal integral scales.

A very large number of individual measurements on mean surface pressure and fluctuating pressures would initially appear to be available. But closer examination shows that few data are for well documented boundary layers and much of the boundary layer data may be systematically in error. In addition pressure measurements on the side and back walls are very sparse.

Pressure Fluctuations Over the Body Surfaces:

Fluctuations in pressure are caused by turbulence in the flow approaching the structure and by flow disturbances generated by the structure itself. The instantaneous pressure acting at a particular point on a structure is thus a function of wind magnitude and direction, roughness characteristics of the local and distant upwind area, overall building shape, and local disturbances to the flow on the structure such as mullions or exposed columns. Because of the random nature of wind direction and amplitude, the local pressure also fluctuates in a random manner. Early measurements of pressure fluctuations on forward facing walls by Dagliesh (1971) on a full scale building and by Cermak and Sadeh (1971) on a model structure revealed that pressure fluctuations had a Gaussian distribution similar to the approach wind. Later Peterka and Cermak (1975) measured pressure fluctuations on lee sides of a model building in the negative mean pressure regions. They found that probability distributions in regions where $Cp_{mean} < -0.25$ were non-Gaussian and consistently had long negative tails. These negative tails are caused by intermittent large negative pressure spikes, possibly caused by movement of reattachment streamlines.

Although extensive proprietary information exists about pressure fluctuations on specific and unique building shapes for design purpose; additional measurements of fluctuating pressures on simple block structures are limited. Kwai, Katsura and Ishizaki (1979) measured pressure fluctuations on the windward wall of two-dimensional square prisms in grid-generated turbulence. They concluded that the pressure spectrum was not linearly related to the approach-wind velocity spectrum, but that pressure fluctuation scales were 1.5 to 2 times larger than those of the velocity fluctuations. The most extensive study of the effects of upstream turbulence on the pressure field of a square prism in a two dimensional flow may have been carried out by Lee (1975). He measured spatial correlations and concluded the vortex-shedding mode contained the highest percentage of the energy, but the percentage was reduced by the turbulence intensity of the approach flow.

Akins (1976) carried out comprehensive measurements of pressure fluctuations over a wide range of buildings and boundary layers in order to isolate relevant geometrical variability on the building

faces. All studies were at a zero angle of attach for the approach wind. Hunt (1981) also measured rms and peak pressure distributions over a cubical building in two boundary layers. The velocity profile and local geometry were found to mainly determine the pressures on the front face of the model, while integral length scale, turbulence intensity and local turbulent share affected the pressures on the other faces. Kareem and Cermak (1984) reported spatio-temporal measurements of fluctuating pressure fields acting on the side faces of a square prism of finite height in boundary-layer flows for zero degree angle of attack winds. They concluded " increased levels of turbulence in the incident flow have a marked influence on the fluctuating pressure field, through modifications which take place in the structure of the separated shear layers. The periodic vortex-shedding process is vitiated in the presence of high levels of turbulence intensity in the incident flow, resulting in redistribution of the energy associated with pressure fluctuations over a wider frequency range." They also found spatial dependence of the pressure fluctuations decreases with an increase in approach flow turbulence. Recently, Stathopoulos and Baskaran (1985) reported mean and fluctuating pressures over roofs on a model block building including the effects of different parapet heights. Such information may help to predict roof paver behavior such as was described by Bienkiewicz and Meroney (1986).

Surface Shear Over the Body Surfaces:

Fluctuating surface shear stresses on the top surface of a simple block type bluff prisms (B/H = 9, L/H = 1 and 2) mounted in thick turbulent boundary layers were completed by Castro and Dianat (1983) and Dianat and Castro (1984). These measurements identified three characteristic separation flow fields--firstly, a body sufficiently long in the axial direction to ensure permanent reattachment of the "roof" shear layer separating from the leading edge; secondly, situations which result in intermittent reattachment; and thirdly, a bodies sufficiently short that reattachment does not occur. They concluded:

a. Roof flows on obstacles are always so unsteady that investigations of the mean flow characteristics and mean pressure distributions cannot be used reliably to infer the direction of mean surface flows;

b. Although rms values of the fluctuating surface shear stress vary much less than the mean; they cannot be used to deduce the locations of critical points; yet maximum rms fluctuating shear values occur near regions of reattachment;

c. Maxima in the rms value of the fluctuating surface pressure also occur near the reattachment point, whether this attachment is of the approach shear layer separating from the leading edge, or of the smaller-scale reverse flow shear layer separating from the trailing edge.

CONCLUSIONS:

Two kinds of measurement programs would be advisable:

a. A program to definitively determine the effect of flow field structure on mean and fluctuating pressures, and

b. A program to accurately document pressures over the anticipated useful size range of buildings and atmospheric boundary layers.

Program to Define Building Aerodynamics Flow Physics:

Mean pressure coefficient distributions alone are not adequate to identify the flow field characteristics of bluff bodies. A well designed measurement program should include measurement of mean and fluctuating pressures, flow visualization, surface shear fluctuations, and pressure-velocity fluctuation correlation measurements.

Spatio-temporal correlation of the approach flow or above-surface velocity fluctuations with surface pressures or forces over small surface areas would be extremely useful. This information would help produce an analytical model for the velocity/pressure admittance functions needed to calculate building forces. The data would also be valuable for predicting uplift and movement forces on roof pavers and stones.

Specific measurements should include:

a. For the approach flow the velocity and turbulence profiles, integral scales over the body height, and spectra over the body height,

b. For pressures the mean, rms, probability distributions, and extreme values over all building faces, and limited spatial correlations in regions of streamline reattachment,

c. For shear the mean, rms, probability distributions, extreme values and limited spatial correlations in regions of streamline reattachment, and

d. Limited spatio-temporal correlations of velocity fluctuations and pressure or shear fluctuations in regions of streamline reattachment.

These measurements should be carried out over rectangular block buildings in body shapes which cover the three reattachment situations (full, intermittent and no reattachment) in boundary layers of at least three roof height turbulence levels (5, 10, and 20%).

Program to Produce Code Information:

Measurements need to be carried out in a broader range of boundary layer and building geometry situations which typify the actual building environment. In particular measurements of building

performance in highly-turbulent urban center under deep atmospheric boundary layers seem to be missing.

Specific measurements should include:

a. Approach wind characteristics of velocity and turbulence profile, integral scale and spectra at roof height and a reference height of 10m, and

b. Mean and fluctuating pressures over all building surfaces reduced to mean, rms, and peak coefficient of pressure values based on wind at roof height.

These measurements should be carried out over rectangular block buildings in body shapes which cover the range of current building practice and known atmospheric boundary layer characteristics. Tentatively this should include a range of Delta/H ratio up to 200 if possible. A parametric study of extreme pressures of the sort described by Gumley (1984) would be useful.

REFERENCES:

Ackert, J. and Egli, J. (1966), "Uber die Verwendug sehr kleiner Modelle fur Winddruck-Versuche, Schweizerische Bauzeitung, Vol 84, No. 1, pp. 3-7. (as seen in Sockel, H. (1984), Aerodynamik der Bauwerke, Vieweg & Sohn, 432 pp.

Akins, R. (1976), "Wind Pressures on Buildings," Ph.D. Dissertation, Civil Engineering, Colorado State University, Report CED76-77REA7 or CER76-77REA-JEC15.

Arie, M., Kiya, M., Tamura, H., Kosugi, M. and Takoka, K. (1975), "Flow Over Rectangular Cylinders Immersed in a Turbulent Boundary Layer," the J. Society of Mechanical Engineers, Vol. 18, No. 125, pp. 1269-1276.

Bachlin, W. (1985), "Belastung von Gebauden durch den Windindudzierten Innendruck,) Insitut fur Hydrologie and Wasserwirtschaft, U. of Karlsruhe, Heft 26, 164 pp.

Bachlin, W., Plate, E.J., and Karmarga, A. (1983), "Influence of the Ratio of Building Height to Boundary Layer Thickness and of the Approach Flow Velocity Profile on the Roof Pressure Distribution of Cubical Buildings,"J. of Wind Engineering and Industrial Aerodynamics, Vol. 11, pp. 63-74.

Bachlin, W., Plate, E.J., and Karmarga, A. (1984), "Response to discussion contribution by A.G. Robins, J. of Wind Engineering and Industrial Aerodynamic, Vol. 17, pp. 161-162.

Baines, W.D. (1963), "Effects of Velocity Distribution on Wind Loads and Flow Patterns on Buildings," Symposium on Wind Effects on Buildings and Structures, National Physical Laboratory, Symposium 16, Teddington, U.K., Vol. I, Paper 6, pp. 198-233.

Castro, I.P. and Dianat, M. (1983), "Surface flow patterns on rectangular bodies in thick turbulent boundary layers," J. of Wind Engineering and Industrial Aerodynamics, Vol. 11, pp. 107-119.

Castro, I.P. and Robins, A.G. (1977), "The flow around a surface-mounted cube in uniform and turbulent streams," J. Fluid Mech., Vol. 79, Part 2, pp. 307-335.

Chien, N., Yin, F., Wang, H.J., Siao, T.T. (1951), "Wind-tunnel Studies of Pressure Distribution on Elementary Building Forms," Iowa Institute of Hydraulic Research, State Univ. of Iowa, Iowa City, 113 pp.

Corke, T.C. and Nagib, H.M. (1979), "Wind Loads on a Building Model in a Family of Surface Layers," J. of Industrial Aerodynamics, Vol. 5, pp. 159-177.

Dagliesh, W.A. (1961), "Statistical Treatment of Peak Gusts on Cladding," J. of the Structural Divison, ASCE, Vol. 97, No. ST9, Paper 8356, pp. 2173-2187.

Davenport, A.G. (1982), "The interaction of wind and structures," Engineering Meteorology, (ed. E.J. Plate), Elsevier, pp. 527-572.

Dianat, M. and I.P. Castro, (1984), "Flucturating Surface Shear Stresses on Bluff Bodies," J. of Wind Engineering and Industrial Aerodynamics, Vol. 17, pp. 133-146.

Frimberger, R. and P. Schmid. (1984), "Messung der Windlasten an einem kubischen Korper im naturlichen Wind und Vergleich der Ergebnisse mit Werten aus verschiedenen Windkanalen," Lehrstuhl fur Stromungsmechanik, Technische U. Munchen, IRB Verlag T1420, 46 pp.

Good, M.C. and Joubert, P.N. (1968), "The Form Drag of Two-Dimensional Bluff-Plates Immersed in Turbulent Boundary Layers," J. Fluid Mech., Vol. 31, Part 3, pp. 547-582.

Gumley, S.J. (1984), "A Parametric Study of Extreme Pressures for the Static Design of Canopy Structures," J. of Wind Engineering and Industrial Aerodynamics, Vol. 16, pp. 43-56.

Hamilton, G.F. (1962), "Effect of Velocity Distribution on Wind Loads on Walls and Low Buildings," Dept. of Mechanical Engineering, U. of Toronto, Report UTME TP 6205, 61 pp.

Hosker, R.P. Jr. (1984), "Flow and Diffusion Near Obstacles," Chapter 7 in Atmospheric Science and Power Production, U.S. Dept of Energy, Report DOE/TIC-27601, (ed. D. Randerson), pp. 241-326.

Hunt, A. (1982), "Wind-tunnel Measurements of Surface Pressures on Cubic Building Models at Several Scales,"J. of Wind Engineering and Industrial Aerodynamics, Vol. 10, pp. 137-163.

Hunt, A. (1981), "Scale Effects on Wind Tunnel Measurements of Wind Effects on Prismatic Buildings," Ph. D. Thesis, Cranfield Institute of Technolgy, 210 pp.

Jensen, M. and Franck, N. (1963), Model-Scale Tests in Turbulent Wind, "Part 2, Phenomena Dependent on the Velocity Pressure, Wind Loads on Buildings," Danish Technical Press, Copenhagen, 172 pp.

Kareem, A. and Cermak, J.E. (1984), "Pressure Fluctuations on a Square Building Model in Boundary-Layer Flows," J. of Wind Engineering and Industrial Aerodynamics, Vol. 16, pp. 17-41.

Katsura, J. (1970), "A Wind Tunnel Test of Pressure Distributions on Box-shaped Models," Wind Loads on Structures, Proceed. of Joint USA/Japan Researach Seminar, Honolulu, Hawaia, October 1970, pp. 97-108.

Kawai, H., Katsura, J. and Ishizaki, H. (1979), "Characteristics of Pressure Fluctations on the Windward Wall of a Tall Building," Proceed. of the 5th Intl. Conference onf Wind Engineering, Fort Collins, Colorado, July, 1979, pp. 519-528.

Kind, R.J. and Wardlaw, R.L. (1982), "Failure Mechanisms of Loose-laid Roof-insulation Systems," J. of Wind Engineering and Industrial Aerodynamics, Vol. 9, pp. 325-341.

Kramer, C. (1975), "Untersuchungen zur Windbelastung von Flachdachern," Der Bauingenieur, Vol. 50, pp. 125-132.

Lee, B.E. (1975), "The effects of turbulence on the surface pressure field of a square prism," J. Fluid Mech., Vol. 69, pp. 263-282.

Leutheusser, H.J. (1965), "Pressure Distribution on a Cube at Various Degrees of Boundary-layer Immersion," Dept. of Mechanical Engineering, U. of Toronto, Report UTME TP 6502, 26 pp.

Leutheusser, H.J. and Baines, W.D. (1967), "Similitude Problems in Building Aerodynamics," J. of the Hydrualics Division, ASCE, Paper 5226, HY3, pp. 35-49.

Lusch, G. and Truckenbrodt, E. (1964), "Windkanaluntersuchungen an Gebauden von rechteckigem Grundriss mit Flach- und Satteldachern," Beichte aus der Bausforschung, Heft 41, Wilhel Ernst & Sohn, Berlin, pp. 23-44.

Meroney, R.N. (1982), "Turbulent diffusion near buildings," Engineering Meteorology, (ed. E.J. Plate), Elsevier, pp. 481-527.

Peterka, J., Kothari, K.M., and Meroney, R.N. (1984), "Wind Flow Patterns about Buildings," J. of Wind Engineering and Industrial Aerodynamics, Vol. , pp. .

Petty, D.G. (1979), "The Effect of Turbulence Intensity and Scale on the Flow Past Square Prisms," J. of Industrial Aerodynamcis, Vol. 4, pp. 247-252.

Plate, E.J. (1982), " Wind tunnel modeling of wind effects in engineering," Engineering Meteorology, (ed. E.J. Plate), Elsevier, pp. 573-640.

Ranga Raju, K.G., Loeser, J., and Plate, E.J. (1976), "Velocity profiles and fence drag for a turbulent boundary layer along smooth and rough flat plates," J. Fluid Mech., Vol. 76, Part 2, pp. 383-399.

Robins, A.G. (1984), "Discussion of Influence of the ratio of building height to boundary layer thickness and of the approach flow velocity profile on the roof pressure distribution of cubical buildings," J. of Wind Engineering and Industrial Aerodynamics, Vol. 17, pp. 159-160.

Sakamoto, H. and Arie, M. (1982), "Flow Around a Cubic Body Immersed in a Turbulent Boundary Layer," J. of Wind Engineering and Industrial Aerodynamics, Vol. 9, pp. 275-293.

Sakamoto, H., Moriya, M., Taniguchi, S., and Arie, M. (1982), "The Form Drag of Three-Dimensional Bluff Bodies Immersed in Turbulent Boundary Layers," J. of Fluid Engineering, ASME, Vol. 104, pp. 326-334.

Scruton, C. and Rogers, E.W.E. (1971), "II. Wind Effects on Buildings and Other Structures," Phil. Trans. Roy. Soe. Lond., A. Vol. 269, pp. 353-383.

Stathopoulos, T. (1975), "Wind Pressure Loads on Flat Roofs," M.S. Thesis, Engineering Science, U. of Western Ontario, London, Ontario, Candada, Boundary Layer Wind Tunnel Laboratory Report No. BLWT-3-1975, 182 pp.

Stathopoulos, T. and Baskaran, A. (1985), Proc. Fifth U. S. National Conference on Wind Engineering, November 6-8, 1985, Texas Tech University, Lubbock, Texas.

Stathopoulos, T. (1981), "Wind Pressure Functions for Flat Roofs," J. of Engineering Mechanics Division, ASCE, Paper 16546, Vol. 107, EM5, pp. 889-905.

Stathopoulos, T., Surry, D., and Davenport, A.G. (1981), "Effective Wind Loads on Flat Roofs," J. of Structures Division, ASCE, Paper 16039, Vol. 107, ST2, pp. 281-298.

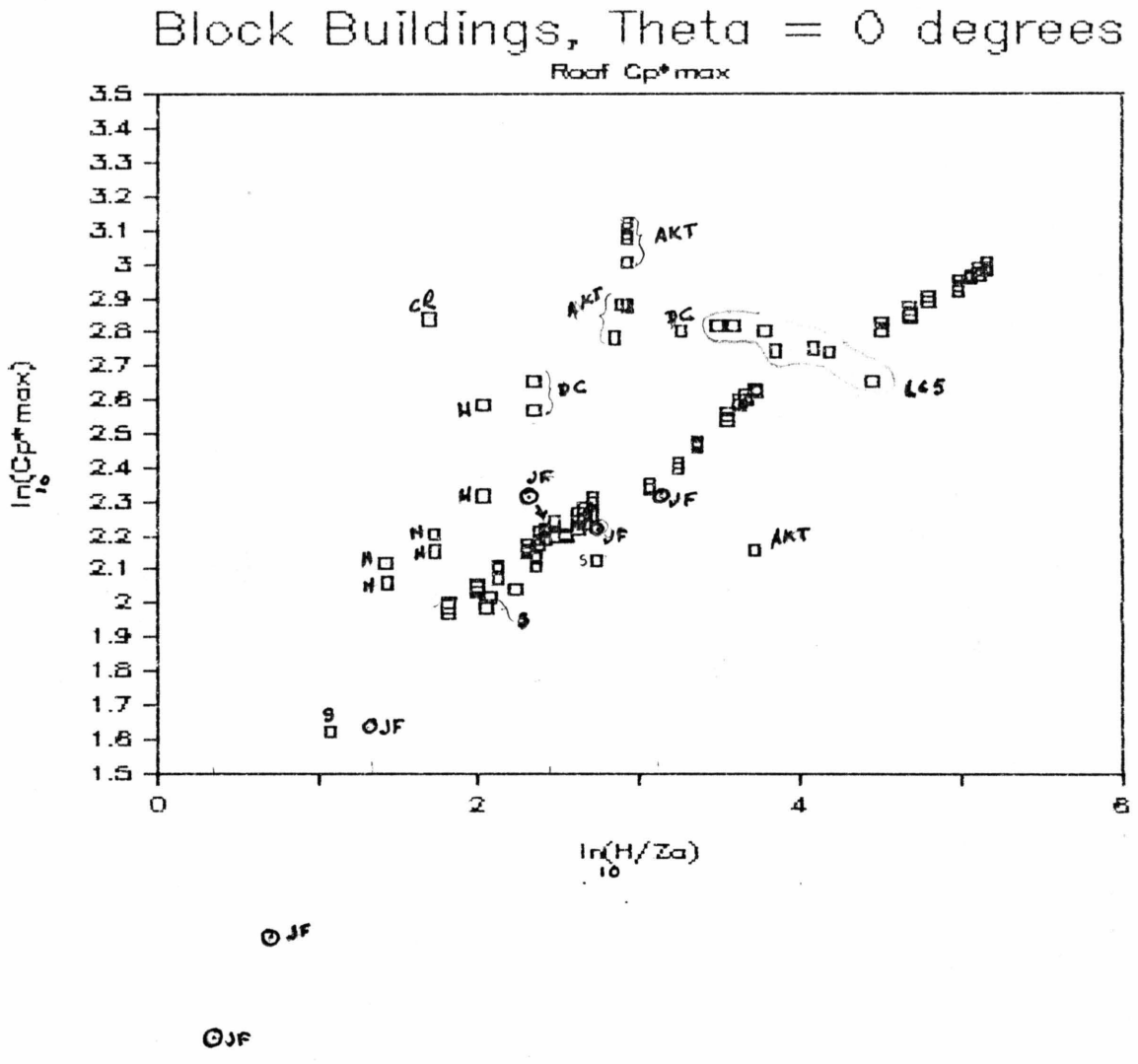

JF

JF

Figure 1

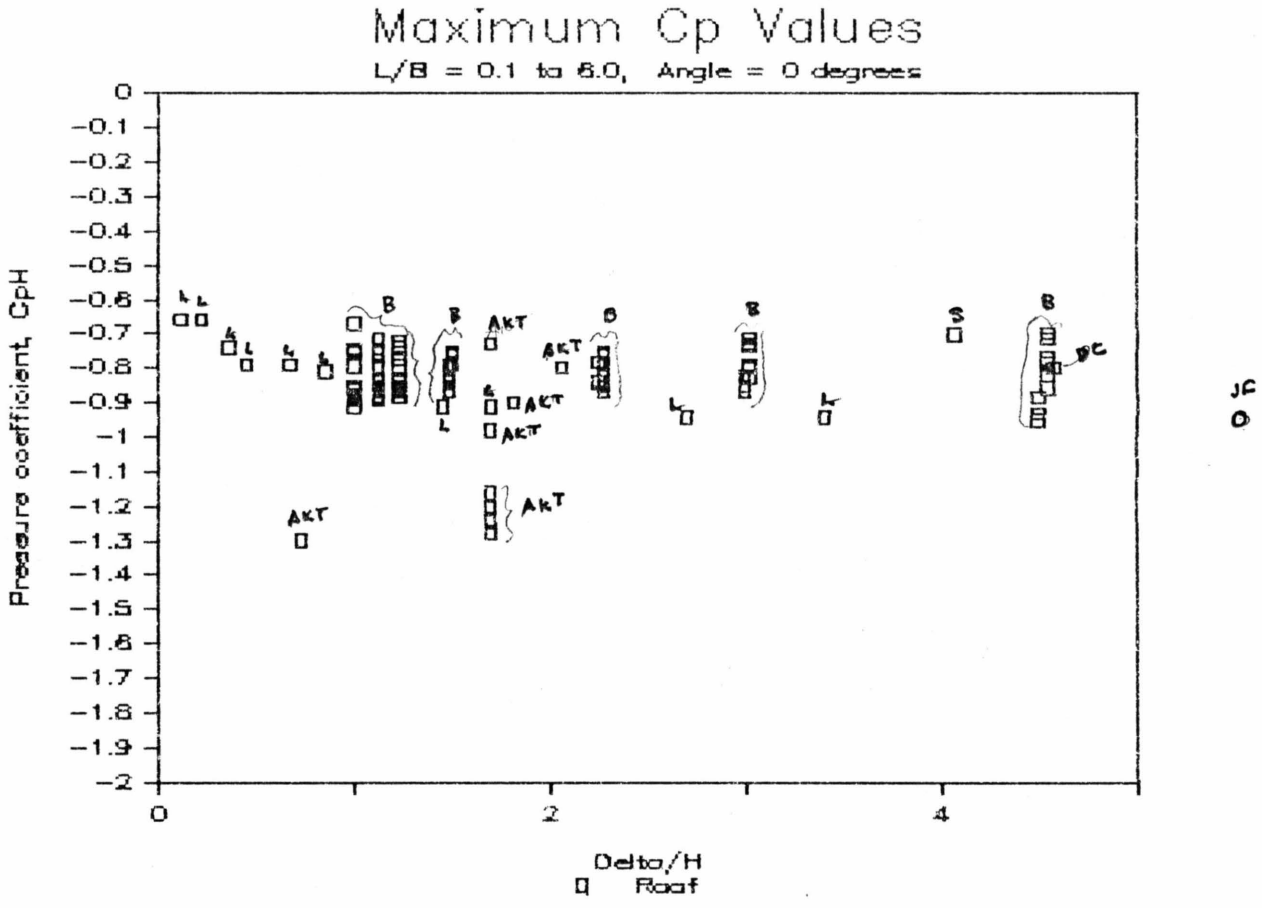
Maximum Cp Values
L/B = 0.1 to 6.0, Angle = 0 degrees
Pressure coefficient, CpH
0
-0.1
-0.2
-0.3
-0.4
-0.5
-0.6
-0.7
-0.8
-0.9
-1
-1.1
-1.2
-1.3
-1.4
-1.5
-1.6
-1.7
-1.8
-1.9
-2
0
2
4
Delta/H
Roof
AKT
JC

Figure 2

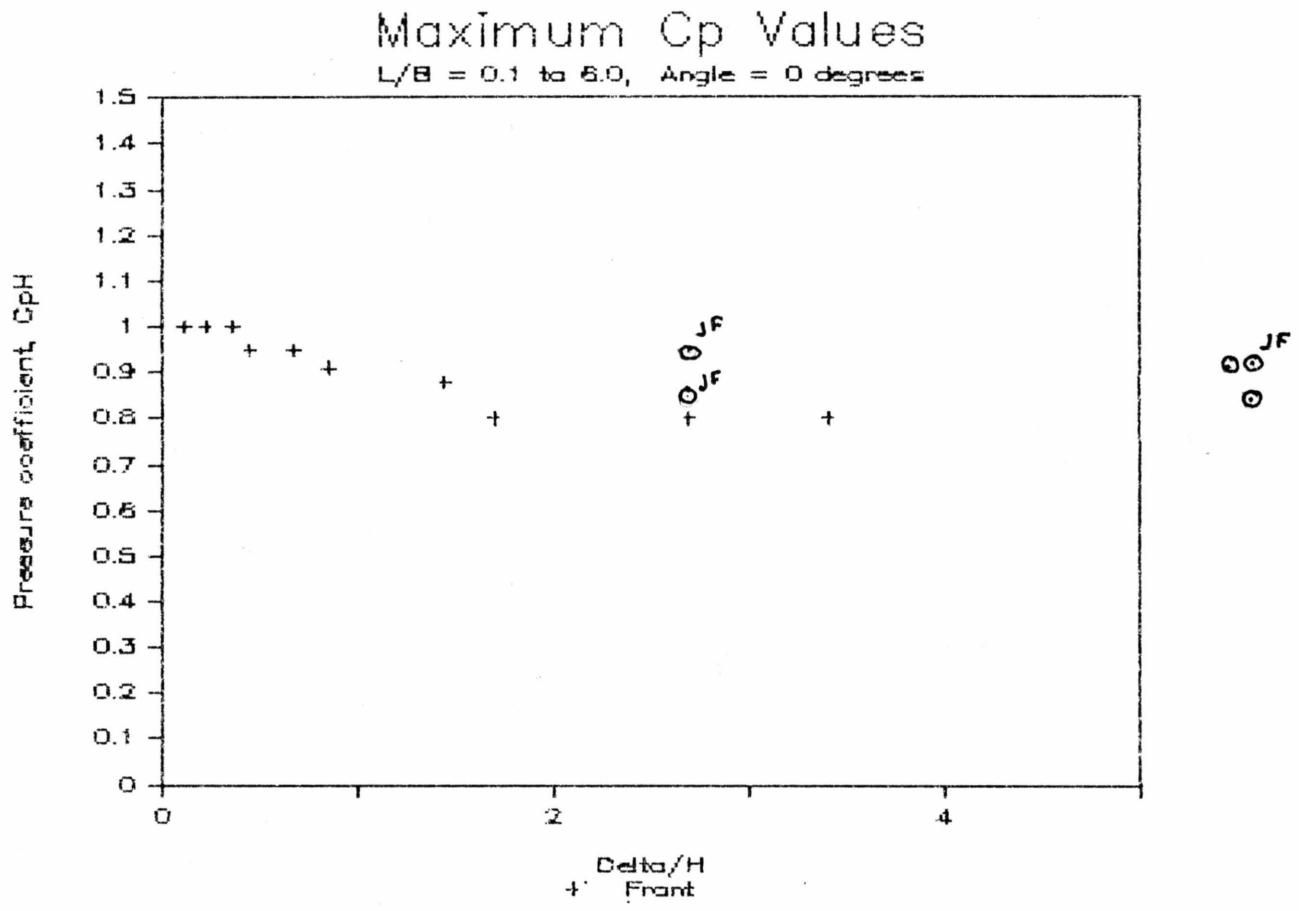

+ Leuthesser 1965

Figure 3

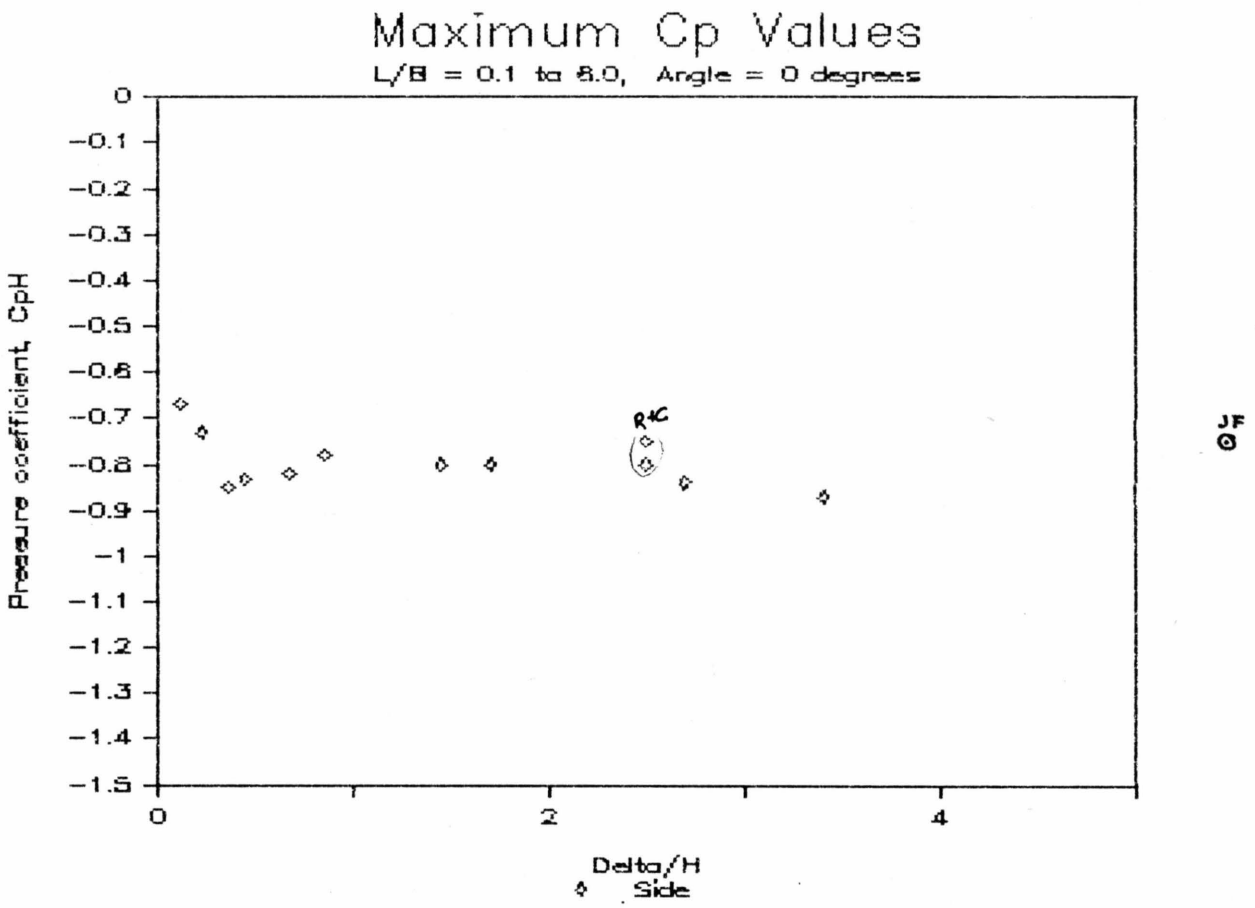

◇ Leutheusser 1965

Figure 4

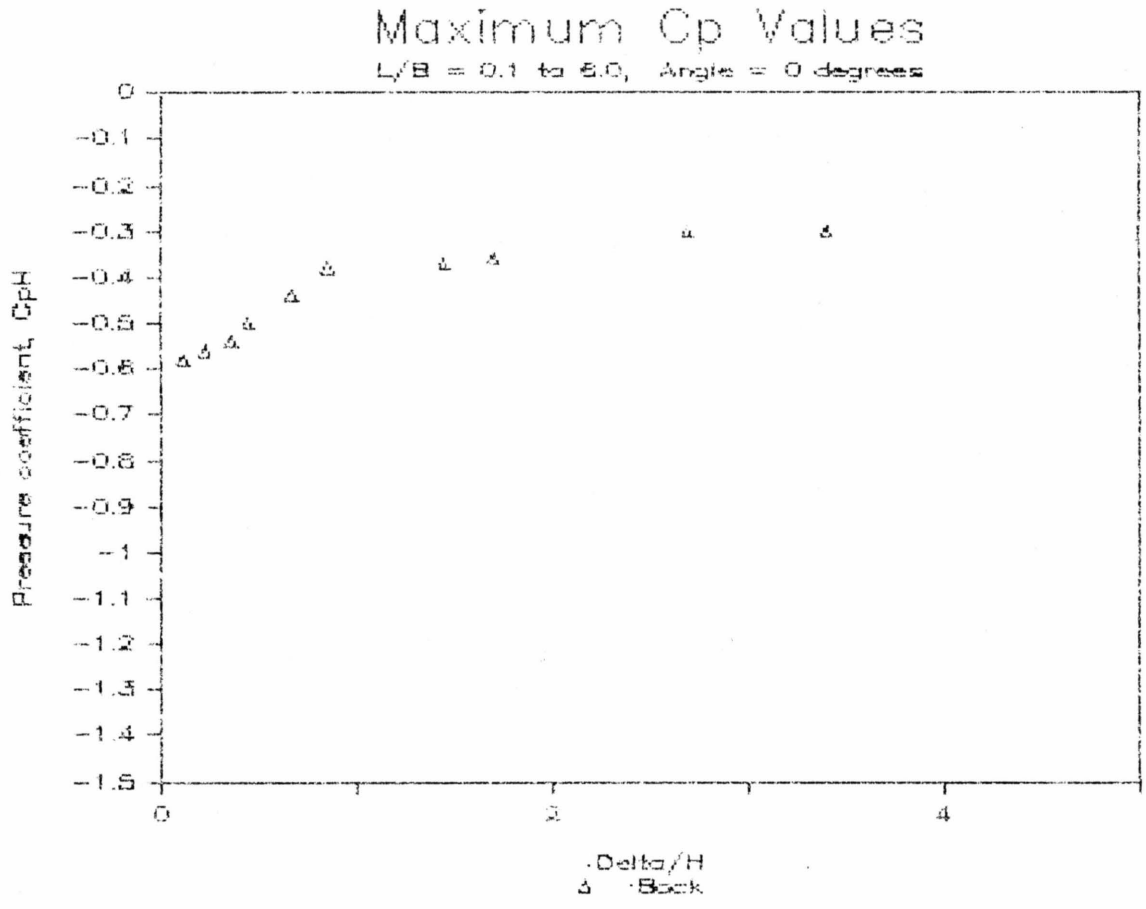

Δ Leuthausser 1965

Figure 5

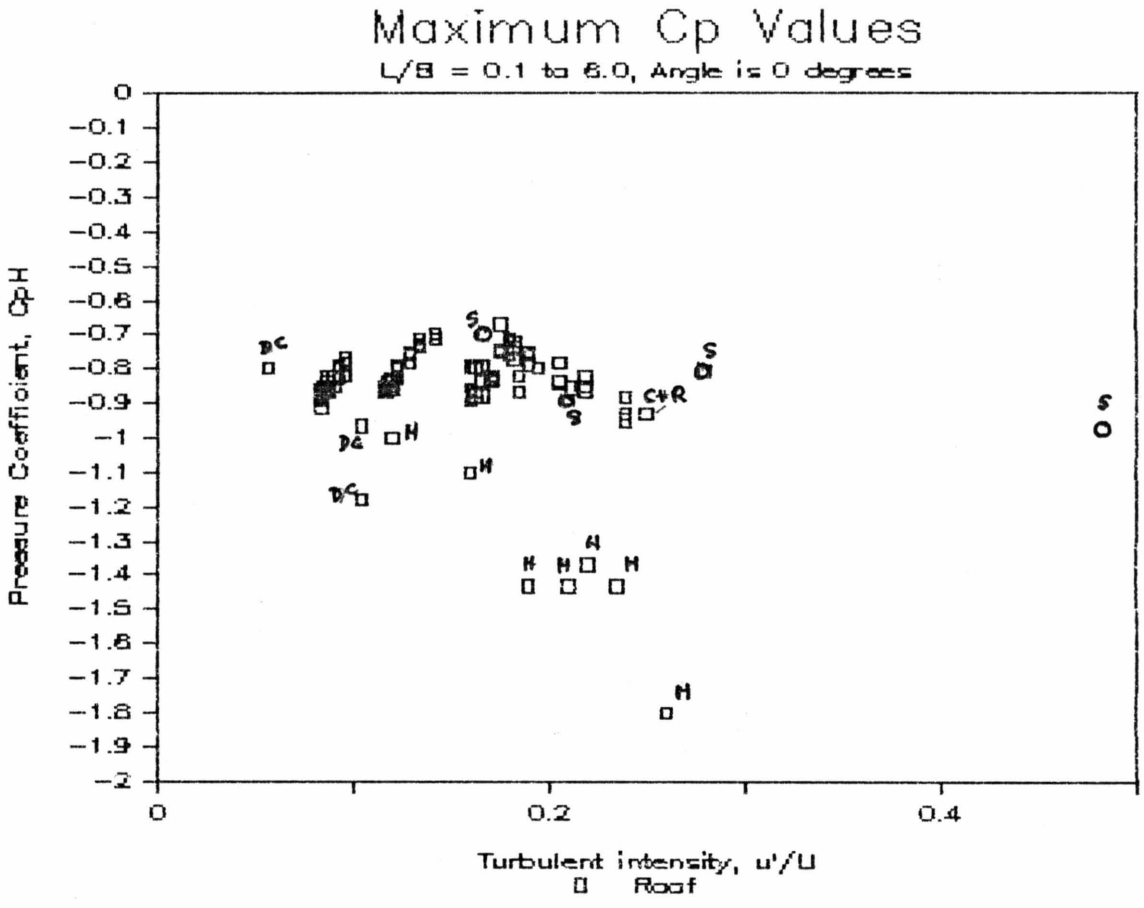

□ Bächlin et al.

$\frac{u'}{u} = 1/\ln z/z_0$

Figure 6

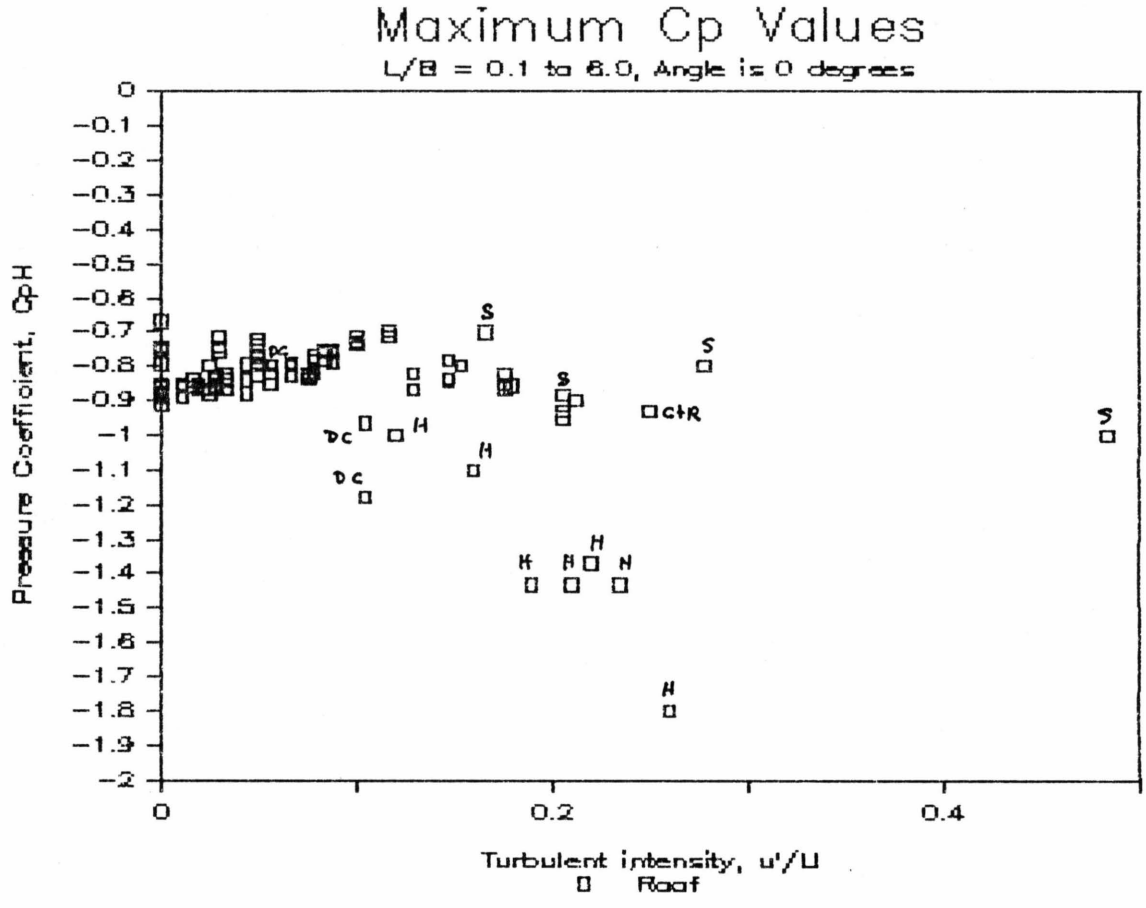

a Bächlin values $\frac{u'}{\bar{u}} = \alpha\left(1 - \frac{H}{\delta}\right)$

Figure 7

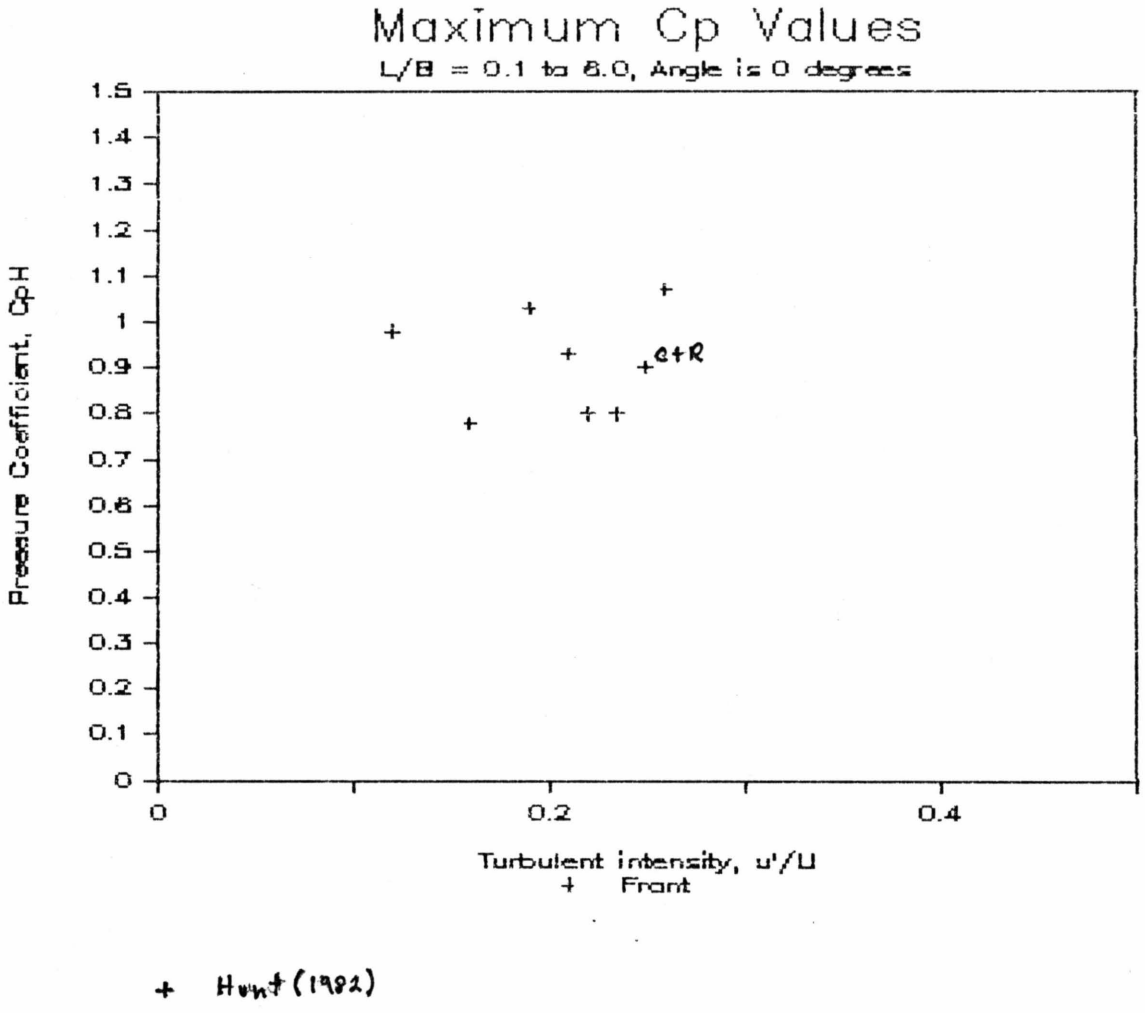
Maximum Cp Values
L/B = 0.1 to 6.0, Angle is 0 degrees
Pressure Coefficient, CpH
1.5
1.4
1.3
1.2
1.1
1
0.9
0.8
0.7
0.6
0.5
0.4
0.3
0.2
0.1
0
0
0.2
0.4
C+R
Turbulent Intensity, u'/U
+ Front
+ Hunt (1982)

Figure 8

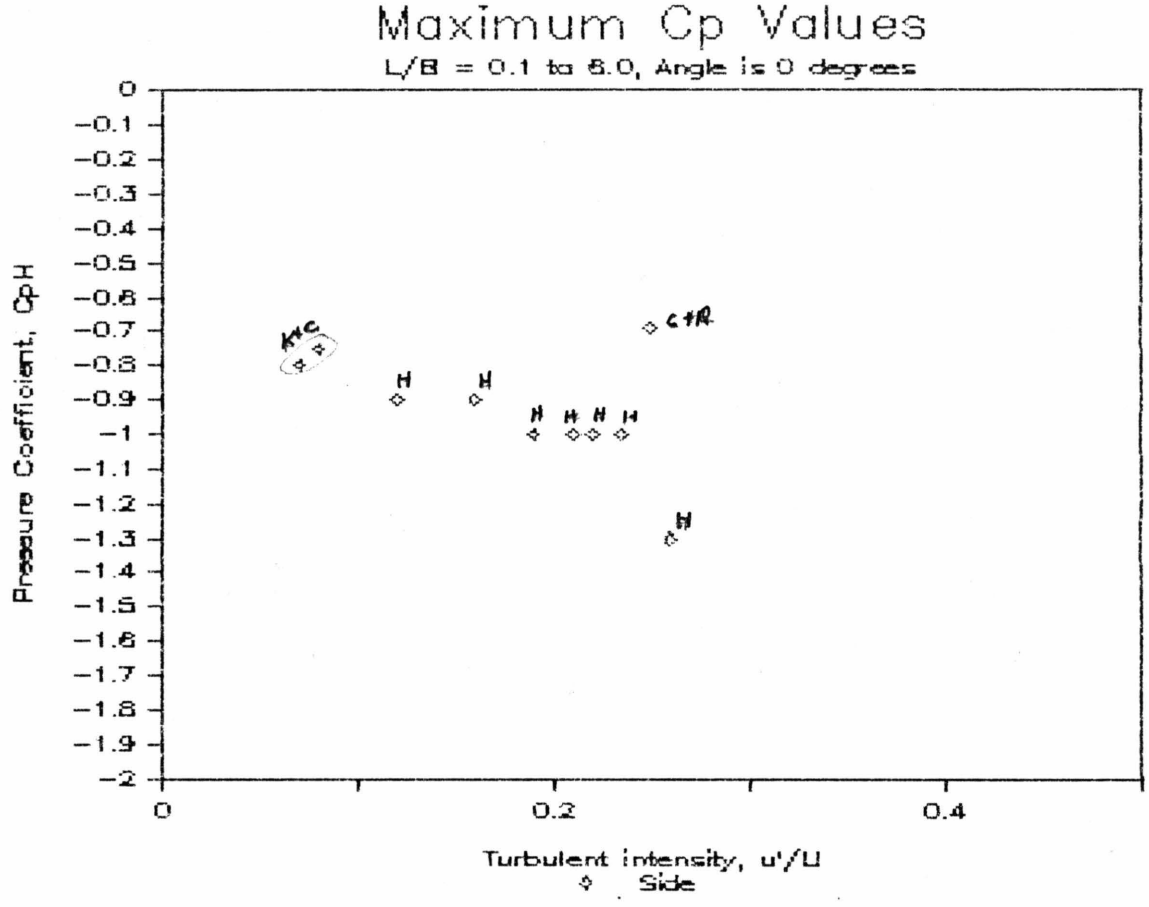
Maximum Cp Values
L/B = 0.1 to 6.0, Angle is 0 degrees
Pressure Coefficient, CpH
0
-0.1
-0.2
-0.3
-0.4
-0.5
-0.6
-0.7
-0.8
-0.9
-1
-1.1
-1.2
-1.3
-1.4
-1.5
-1.6
-1.7
-1.8
-1.9
-2
0
0.2
0.4
Turbulent Intensity, u'/U
Side
C+R
H

Figure 9

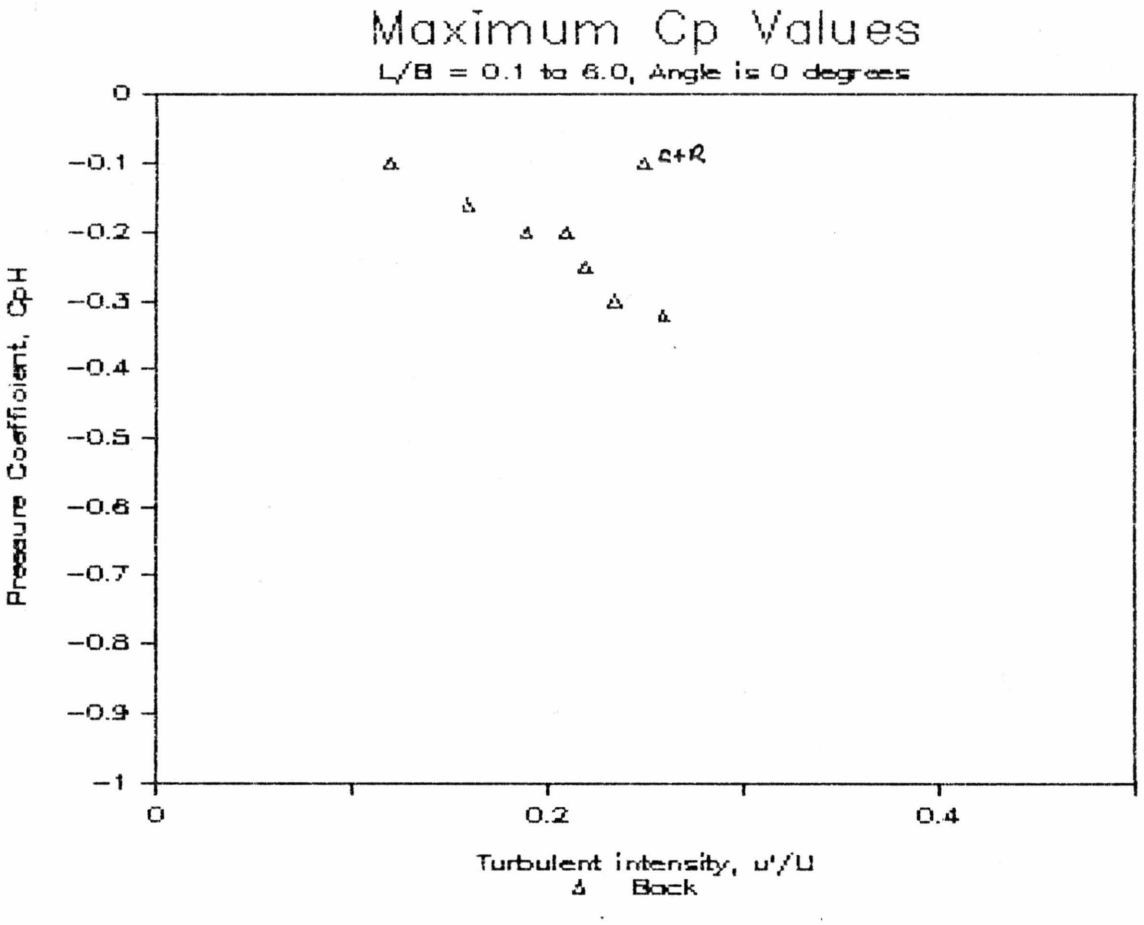
Maximum Cp Values
L/B = 0.1 to 6.0, Angle is 0 degrees
Pressure Coefficient, CpH
0
-0.1
-0.2
-0.3
-0.4
-0.5
-0.6
-0.7
-0.8
-0.9
-1
0
0.2
0.4
C+R
Turbulent intensity, u'/U
Δ Back
▲ Hunt 1982

Figure 10

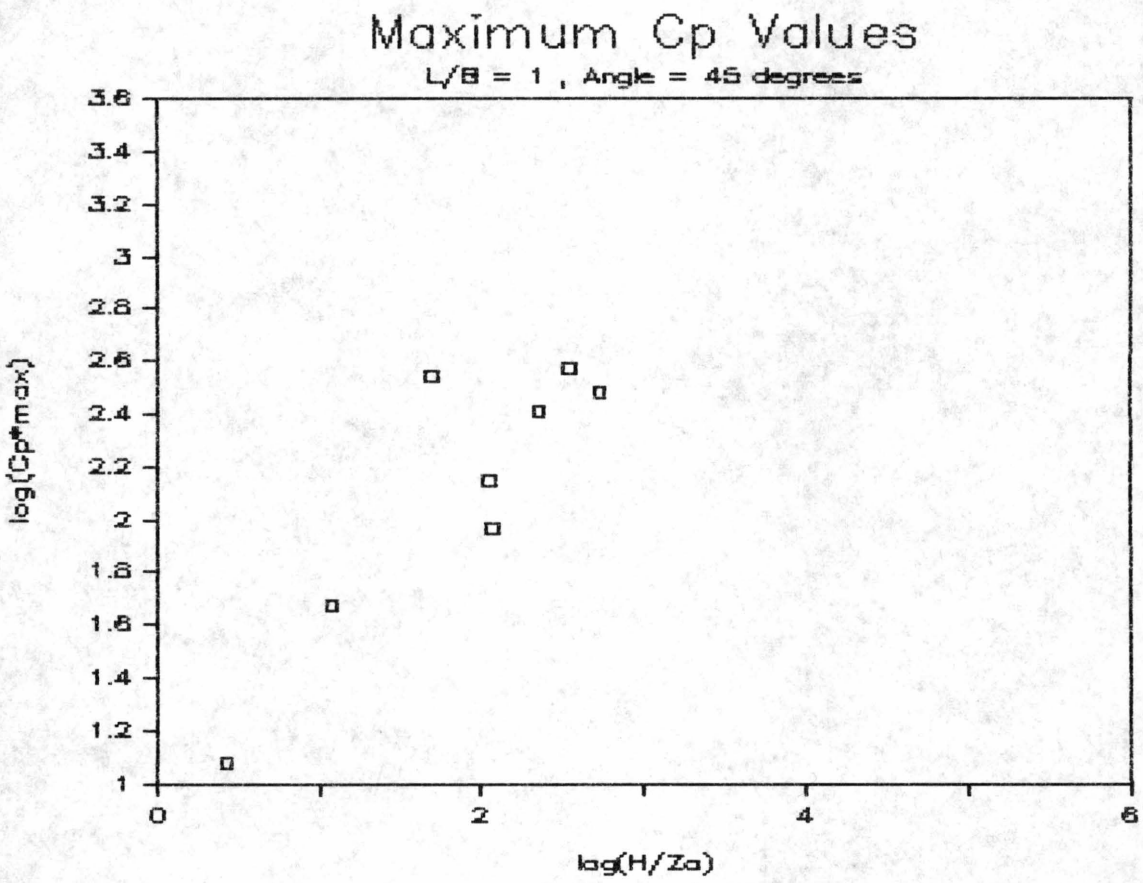

Roof values

Figure 11

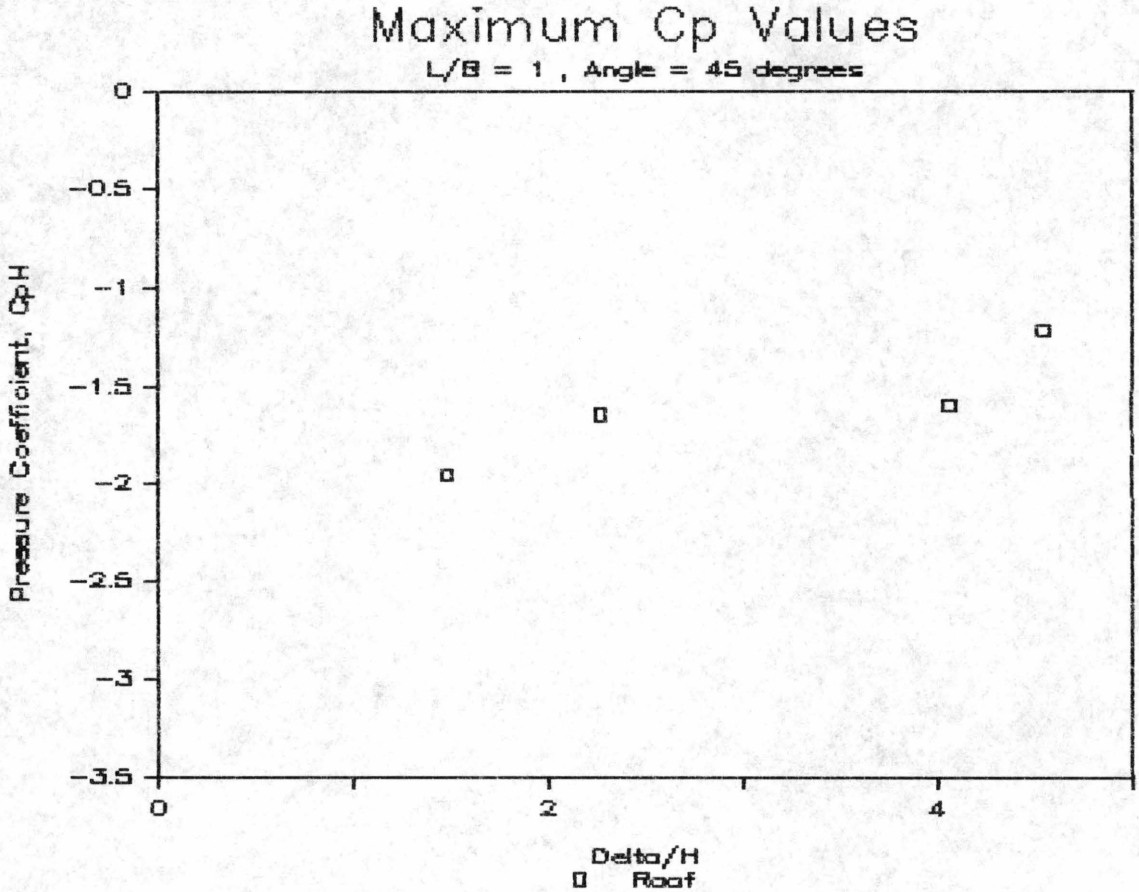
Maximum Cp Values
L/B = 1 , Angle = 45 degrees
Pressure Coefficient, Cp,H
0
-0.5
-1
-1.5
-2
-2.5
-3
-3.5
0
2
4
Delta/H
Roof

Figure 12

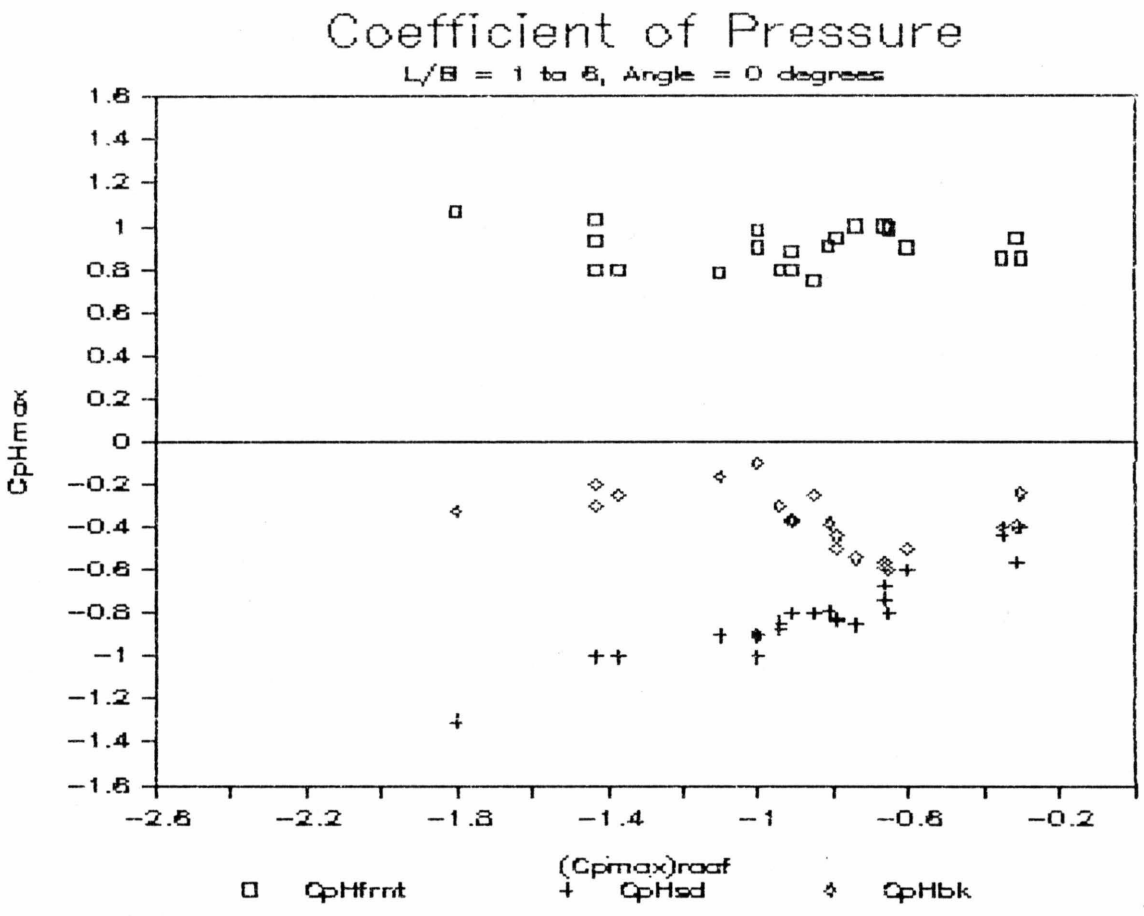
Coefficient of Pressure
L/B = 1 to 6, Angle = 0 degrees
CpHmax
1.6
1.4
1.2
1
0.8
0.6
0.4
0.2
0
−0.2
−0.4
−0.6
−0.8
−1
−1.2
−1.4
−1.6
−2.6
−2.2
−1.8
−1.4
−1
−0.6
−0.2
(Cpmax)roof
CpHfrnt
CpHsd
CpHbk

Figure 13

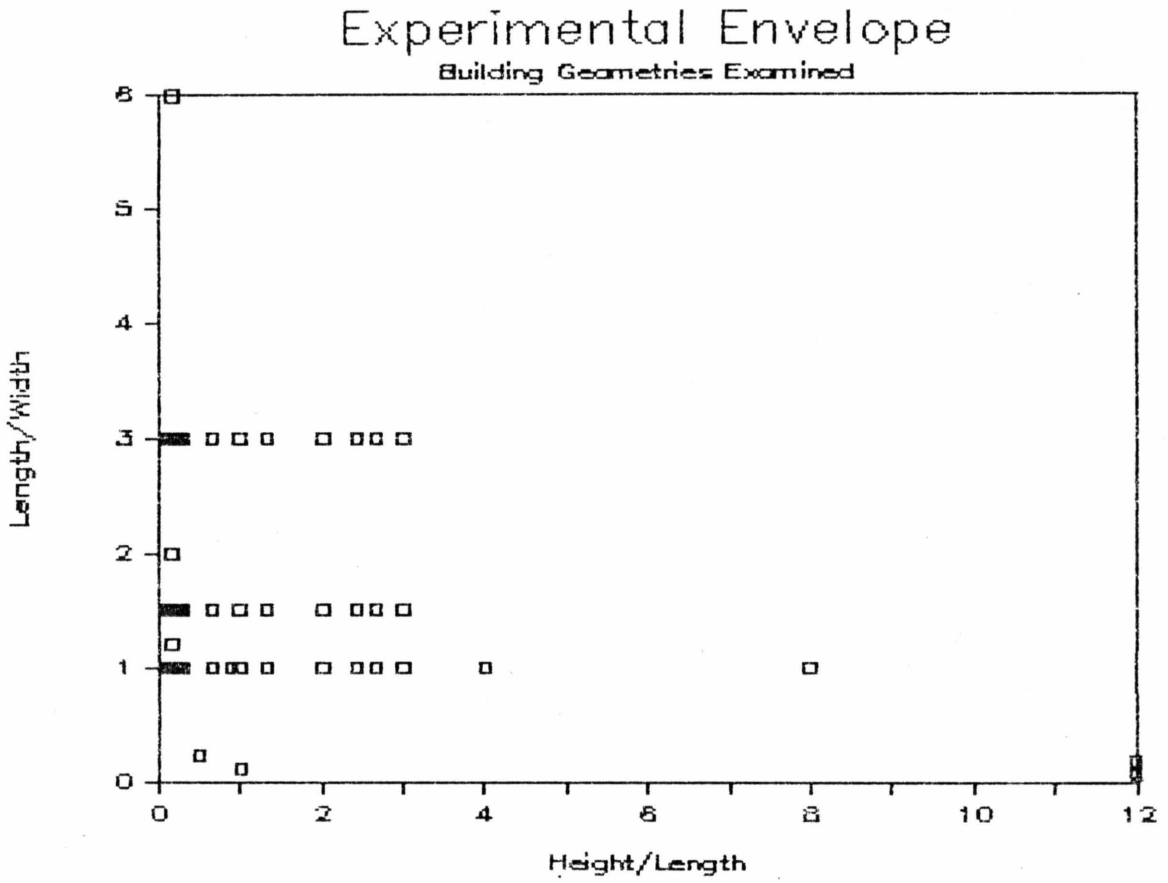
Experimental Envelope
Building Geometries Examined
Length/Width
Height/Length
0
1
2
3
4
5
6
0
2
4
6
8
10
12

Figure 14

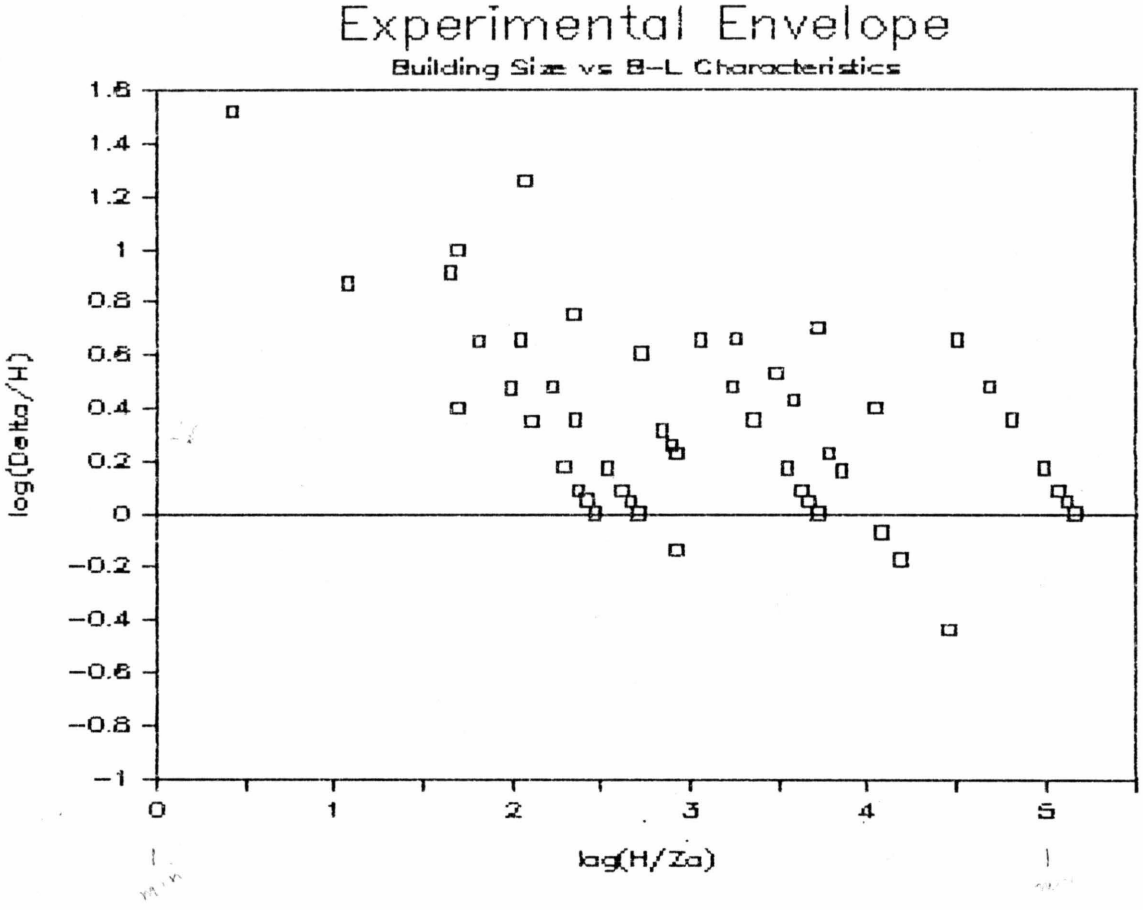
Experimental Envelope
Building Size vs B-L Characteristics
log(Delta/H)
log(H/Zo)
1.6
1.4
1.2
1
0.8
0.6
0.4
0.2
0
-0.2
-0.4
-0.6
-0.8
-1
0
1
2
3
4
5

Figure 15

APPENDIX A

Apparent Correlation of Data Produced by Using Correlated Variables in Ordinate and Abscissa Parameters

Even a random number constrained to vary between say 0.5 to 1.0 will give the impression of strong correlation to a totally independent parmeter when both the ordinate and abscissa are scalled by functions of the independent parameter. Given R a random variable, then a highly correlated plot with some independent variable say A may be produced by plotting:

$$Rf_1(A) \text{ versus } f_2(A).$$

In particular it is inappropriate to infer high correlation between fluid mechanics type parameters in turbulent boundary layers if a variable of interest is made dimensionless by the friction velocity, u_*, generally a small parameter when data is plotted against boundary layer depth, H, divided by some small scaling length such as roughness length, Z_o. Correlation or a biased plot occurs because $U/u_* = f(H/Z_o)$.

There indeed may be variance of the dependent parameter explained by a functional relationship between such a scaled grouping and H/Z_o. However, if 90% or more of the variance is explained by the velocity relationship above, then it is difficult to separate such correlation from random scatter of experimental data.

Consider examples selected from Ranga Raju et al. (1976) and Bachlin et al. (1982). First, in Ranga Raju et al. the drag of a two-dimensional sharp-edged fence is plotted dimensionally as $C_{Do} = F/(U_\infty^2 H/2)$ versus Delta/H in their Figure 1. Let us rescale the dependent parameter as follows:

$$C_{Do} = F/(\rho U_H^2 H/2)\ (U_H/U^\infty)^2, \text{ but since}$$

$$U_H/U^\infty = (H/\delta)^\alpha, \text{ then}$$

$$C_{Do} = C_{DH}\ (H/\delta)^{2\alpha}.$$

Since $= 10^{1/2}\ (u_*/U_\infty)$, then for the data considered $-0.238 < \alpha < -0.22$. On Figure A-1 extracted from Ranga Raju et al. is a comparison plot of the function A-1 above against the data assuming that $C_{DH} = 0.9$. A similar plot can be produced using the well known log-law expression for the velocity profile. The agreement of line and data are excellent, suggesting that almost all data variability is explained by velocity profile variation.

Second, consider the corrected data for Good and Joubert (1968) provided by Ranga Raju et al. in their Figure 3. In this case $C_o^* = F/(\rho u_*^2 H/2)$ is plotted versus $H^+ = u_* h/\nu$. Let us again rescale the dependent variable as follows:

$$C_o^* = F_{Do}/(\rho U_H^2 H/2)\ (U_H/u_*)^2, \text{ but}$$

$$U_H/u_* = 1/k\ \ln(Hu_*/\nu) + B, \text{ where } k = 0.38 \text{ and } B = 2.3, \text{ or}$$

$$= 1/k\ \ln(10\ H^+), \text{ then}$$

$$C_o^* = C_{DH}\ (1/k\ \ln(10\ H^+)^2.$$

Figure A-2 extracted from Ranga Raju et al. compares the Good and Joubert data against the relation above. Notice that the velocity expression explains almost all the variance shown by the data. Within eaxperimental scatter one may say that C_{DH} must be a constant.

Finally, for the Ranga Raju et al. paper consider their Figure 14 where C_o^* is plotted versus H/Z_o. Following the same procedure, consider a recasting of the definition of the dependent variable:

$$C_o^* = F_{Do}/(\rho\ U_H^2 H/2)\ (U_H/u_*)^2, \text{ but now}$$

$$U_H/u_* = 1/k\ \ln(H/Z_o), \text{ then}$$

$$C_o^* = C_{DH}\ (1/k\ \ln(H/Z_o))^2.$$

Figure A-3 extracted from Ranga Raju et al. compares their data as well as the Good and Joubert Data to the relation above. Again the comparison is strikingly good when $C_{DH} = 0.9$. If one is commited to the power law approach an alternative equation can be derived as follows:

$$C_o^* = C_{DH}\ (Z_o/\delta)^{2\alpha}\ (H/Z_o)^2\ /Cf, \text{ where}$$

$$Cf = 0.1\ \alpha^2 \text{ and } Z_o/\delta = 0.15\ \exp(-1/\alpha), \text{ so that}$$

$$C_o^* = C_{DH}\ (0.1\ \alpha^2)^{-1}\ \exp(-2)\ (0.15)\ 2\alpha\ (H/Zo)\ 2\alpha.$$

Figure A-4 displays this new correlation. If one limits the plot to the u_*/U_1 ranges and H/Z_o ranges provided by Ranga Raju et al., then the appearance of correlation against only H/Z_o exists. One wonders if a greater range of data, ie. cases where $\alpha = 0.005$ and $H/Z_o < 1000$ would show much greater data spread as suggested by the curves.

Finally consider the plot of (Cp_*) roof max versus H/Z_o prepared by

Bachlin et al. (1982) in their Figure 7. (Henceforth, let this parameter be designated by C_* for compactness.) Reformulate the dependent parameter as follows:

$$C_* = -p_{max}/(\rho U_H^2/2)\ (U_H/u_*)^2/Cf, \text{ where}$$

again Cf and $Z_o/$ are defined as in the manipulation directly above, then

$$C_* = Cp_H\ \ (0.2\ \alpha 2)-1\ \exp\ (-2)\ (0.15)\ 2\alpha\ (H/Z_o)2\alpha.$$

Figure A-5 displays this new correlation. If one limits the plot to the power law coefficient and H/Z_o ratio ranges provided by Bachlin et al., then then appearance of a correlation C_* proportional to $(H/Z_o)^{0.3}$ exists which agrees with the empirical expression proposed in their paper. In this case one need on limit the Cp_H variation to the region 0.77-0.93 to obtain almost perfect correlation. The inidividual data sets actually seem to agree better with the slopes produced by the biased correlation than the proposed 0.29 slope. If one prefers a log-law type correlation, then use:

$$C_* = Cp_H\ (1/k\ \ln(H/Z_o))^2.$$

The coefficient Cp_H does vary systematically with H/δ or H/Z_o, but these plots shrink the ordinate and stretch the abscissa so much, that it is not possible to differentiate the variation from data scatter on such a chart. In conclusion, it would appear better to avoid dimensionless groups for pressure coefficient or drag force which are not of the O(1) in magnitude.

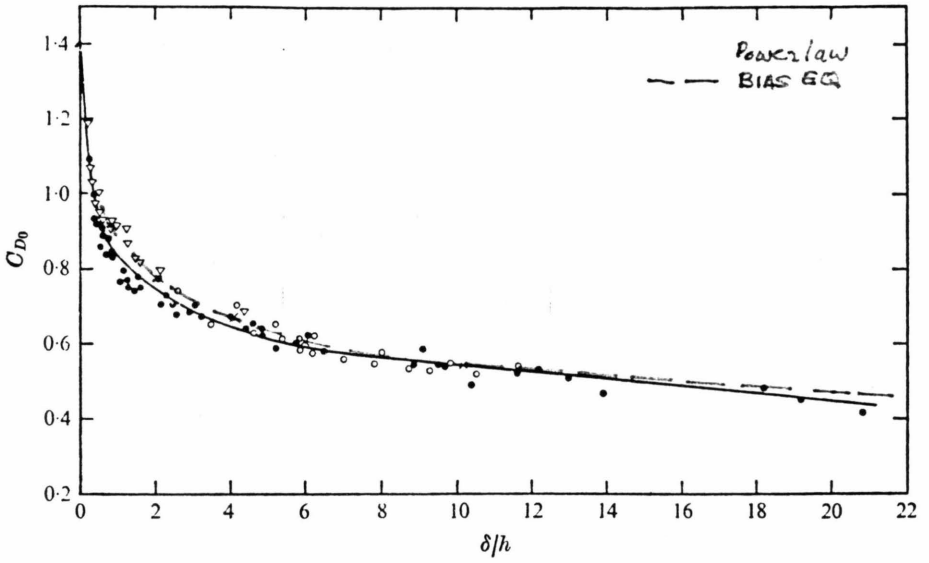

IGURE 1. Drag coefficient of a two-dimensonal fence on a smooth plate.

Source	▽ Ranga Raju & Garde	○ Plate	● Good & Joubert	▲ Arie & Rouse
D(cm)	32.40	183.0	91·50	—
D/h	4·0–32·4	36·0–72·0	9·9–288·0	—

to u_*h/ν at values of $u_*h/\nu \leqslant 10^3$; at higher values of u_*h/ν, C^* was shown to be dependent on both u_*h/ν and u_*/U_0 (for the data of Good & Joubert this bound on u_*h/ν corresponded to $h/\delta \leqslant 0{\cdot}4$–$0{\cdot}5$). But significantly, the data at high u_*h/ν values correspond to the larger fences, for which blockage corrections would be large, and it would be interesting to test the validity of the above conclusion after correcting the results for blockage effects.

Ranga Raju & Garde (1970) evolved a correction for blockage for normal plates with symmetrical rear splitter plates in a uniform stream. Their results are shown in figure 2 and the blockage correction can be written as

$$C_{D0} = C_D(1-h/D)^{2\cdot85}, \tag{2.5}$$

where C_D is the uncorrected drag coefficient and D is the depth of the unobstructed stream. In terms of the drag forces, this equation can be written as

$$F_{D0} = F_D(1-h/D)^{2\cdot85}. \tag{2.6}$$

The applicability of this blockage correction can be investigated for fences in boundary layers by using available data. Examination of (2.1) shows that if fences of different heights are tested in a boundary layer holding δ/h and U_0h/ν constant, and if the values of C_{D0} obtained by using (2.5) remain the same for all these fences, then the blockage correction can be considered valid for fences in the boundary layer also. Table 1, which is based on data collected by Ranga Raju (1967), clearly shows that, for approximately constant values of U_0h/ν and

Fig. A-1

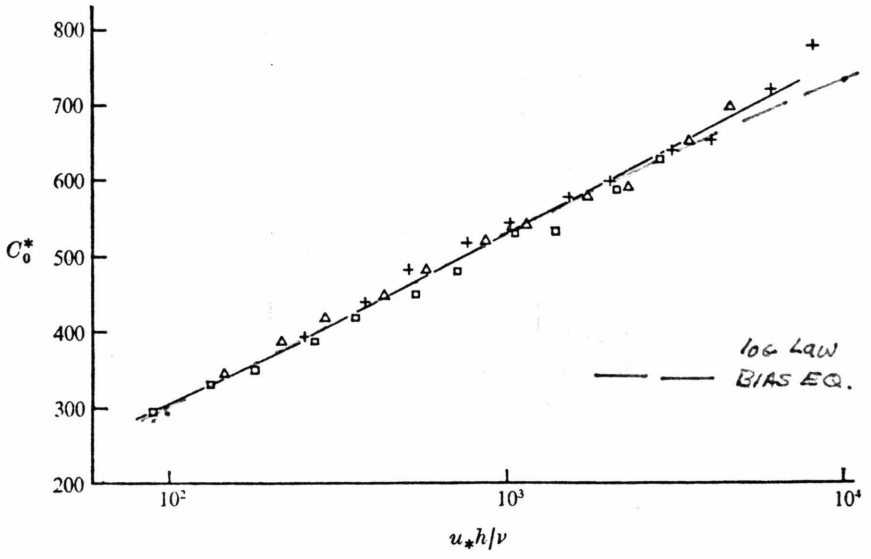

FIGURE 3. Good & Joubert data on smooth walls after blockage correction.
+, $u_*/U_0 = 3{\cdot}48 \times 10^{-2}$; Δ, $u_*/U_0 = 3{\cdot}60 \times 10^{-2}$; □, $u_*/U_0 = 3{\cdot}75 \times 10^{-2}$.

The similarity between (2.7) and (2.8) is obvious when one considers that the variation of C_D with h/D is small at low h/D. Equation (2.7) implies an additive correction. An additive correction is justified if the upstream pressure is unaffected by blockage. However, Ranga Raju & Garde (1970) have shown that the upstream pressure is in fact affected by blockage, though only slightly, at high h/D. In such cases the multiplicative form of blockage correction, viz. (2.5), may be justified. As shown by Ranga Raju & Garde (1970), (2.5) is in excellent agreement with (2.8) over a large range of h/D. In the light of this result and also in view of the applicability of (2.5) to bodies placed in boundary-layer flow, this equation has been used in the present study despite its empirical form.

The data of Good & Joubert (1968) were adjusted accordingly, and the corrected drag coefficient C_0^*, defined as

$$C_0^* = F_{D0}/(\tfrac{1}{2}h\rho u_*^2), \tag{2.9}$$

has been plotted against $u_* h/\nu$ in figure 3. It may be seen that within experimental scatter C_0^* and $u_* h/\nu$ are uniquely related over the entire range of $u_* h/\nu$, but the range of u_*/U_0 values is too small to permit the conclusion that this ratio really has no influence on the drag coefficient.

3. Scope of present work

One of the objectives of the present study was to carry out experiments over a relatively large range of u_*/U_0 and establish clearly whether this parameter is indeed unimportant as figure 3 seems to show. The experiments were performed such that the values of u_*/U_0 for the combined data of the authors and of Good & Joubert range from $3{\cdot}5 \times 10^{-2}$ to $6{\cdot}5 \times 10^{-2}$. Furthermore, it was desired to

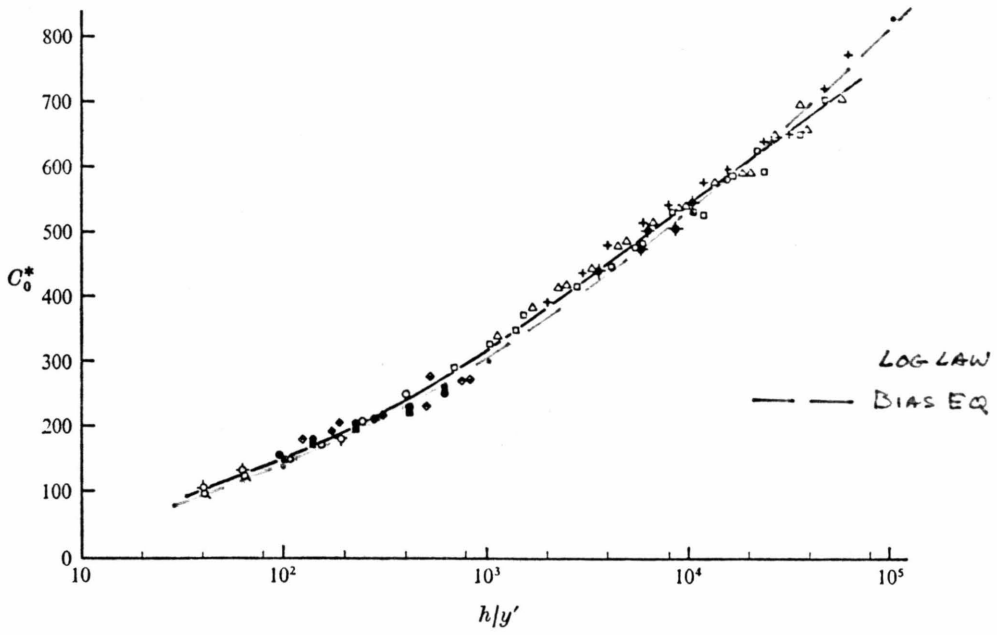

FIGURE 14. Form-drag coefficient of two-dimensional fence in a turbulent boundary layer.

Source	Present		Good & Joubert			Present						
$(u_*/U_0) \times 10^2$	4·42	4·00	3·75	3·60	3·48	5·90	5·26	6·45	6·11	5·92	5·58	5·40
Boundary type	*S*	*S*	*S*	*S*	*S*	*T*	*T*	*R*	*R*	*R*	*R*	*R*

in the outer region of the boundary layer) has no direct influence on the drag on the fence. Also, the ratio δ/h does not enter as a parameter even though for some runs the fence height was larger than the nominal thickness of the boundary layer. The range of δ/h for the data plotted in figure 14 is indeed quite large, from less than one to over twenty. It follows that only that part of the velocity profile which is close to the ground affects the separation of the boundary layer upstream of the fence, the velocity of the separating streamline at the edge of the fence (and consequently the pressure distribution), and the drag on the fence. On the other hand, the parameter u_*/U_0 has no influence on the drag on the fence. The region of overlap of the smooth- and rough-wall data is small (though not that of the data in the transition region) and further studies on a rough wall at large h/y' would be helpful in proving the significance of the parameter h/y'. Nevertheless the data in figure 14 do indicate strongly that the drag coefficient of a two-dimensional fence is uniquely related to h/y'. In generalizing this result one may infer that such a relation also exists for geometrically similarly shaped bluff bodies with sharp edges, provided their dimension in the flow direction is not large enough to cause reattachment of the boundary layer on the body itself. Should this conclusion be verified from studies on some such bodies, the modelling of such bluff bodies in turbulent boundary layers for the estimation of the drag on the

body requires onl
has thus furnishe
of the modelling

7. Conclusions

The characteris
for rough, smooth
The form-drag c
boundary layer u
that the velocity
on the drag of th

The authors be
for modelling the
modelling of wind
enough values th
structure has sha
must be the sam
experiments yiel
coefficient is inde
restricted to ratio
which is customa
As a consequence,
on a model in whi
over the height of
geometry preclud
structure itself.

The first autho
Humboldt founda
III in Karlsruhe.

ARIS, M. & ROUSE,
CLAUSER, F. H. 195
COLES, D. 1956 *J.*
GOOD, M. C. & JOU
JENSEN, M. & FRA
Copenhagen: D
MASKELL, E. C. 196
PLATE, E. J. 1964
PLATE, E. J. 1971
RANGA RAJU, K. G.
RANGA RAJU, K. G.
ROTTA, J. C. 1962
SCHLICHTING, H. 19
SMITH, D. W. & WA

Fig
4-3

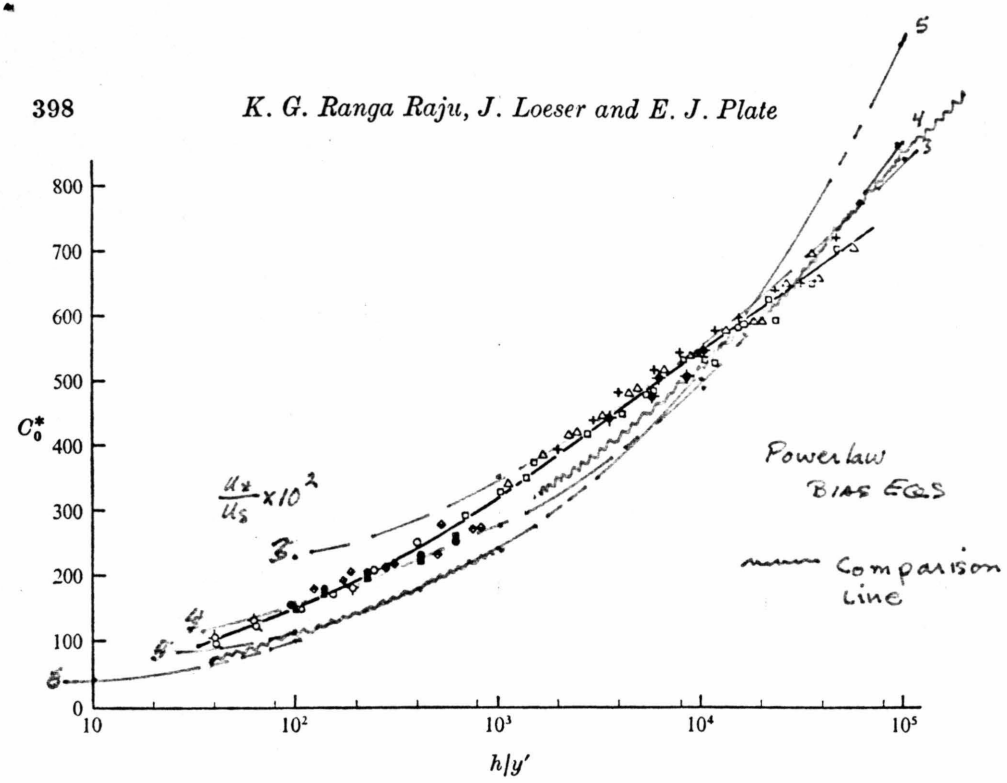

FIGURE 14. Form-drag coefficient of two-dimensional fence in a turbulent boundary layer.

Source	Present		Good & Joubert			Present						
$(u_*/U_0) \times 10^2$	4·42	4·00	3·75	3·60	3·48	5·90	5·26	6·45	6·11	5·92	5·58	5·40
Boundary type	*S*	*S*	*S*	*S*	*S*	*T*	*T*	*R*	*R*	*R*	*R*	*R*

in the outer region of the boundary layer) has no direct influence on the drag on the fence. Also, the ratio δ/h does not enter as a parameter even though for some runs the fence height was larger than the nominal thickness of the boundary layer. The range of δ/h for the data plotted in figure 14 is indeed quite large, from less than one to over twenty. It follows that only that part of the velocity profile which is close to the ground affects the separation of the boundary layer upstream of the fence, the velocity of the separating streamline at the edge of the fence (and consequently the pressure distribution), and the drag on the fence. On the other hand, the parameter u_*/U_0 has no influence on the drag on the fence. The region of overlap of the smooth- and rough-wall data is small (though not that of the data in the transition region) and further studies on a rough wall at large h/y' would be helpful in proving the significance of the parameter h/y'. Nevertheless the data in figure 14 do indicate strongly that the drag coefficient of a two-dimensional fence is uniquely related to h/y'. In generalizing this result one may infer that such a relation also exists for geometrically similarly shaped bluff bodies with sharp edges, provided their dimension in the flow direction is not large enough to cause reattachment of the boundary layer on the body itself. Should this conclusion be verified from studies on some such bodies, the modelling of such bluff bodies in turbulent boundary layers for the estimation of the drag on the

Fig. A-5

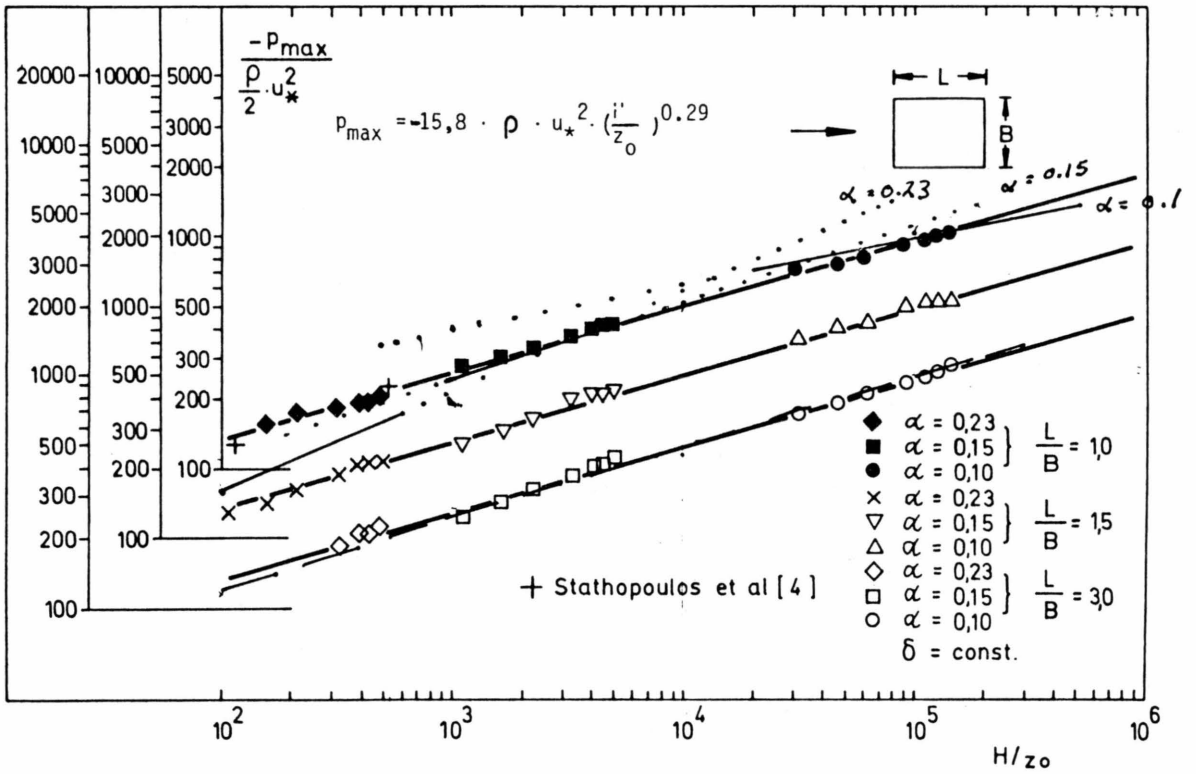

Fig. 7: The relation between p_{max} and the parameters z_o and u_* ——— log law

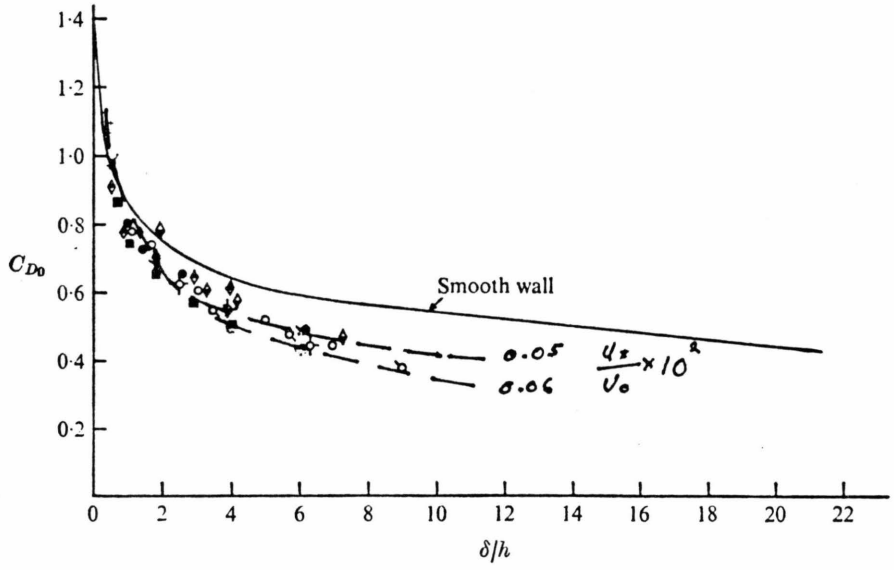

FIGURE 13. C_{D0} *vs.* δ/h for gravel-coated walls.

$(u_*/U_0) \times 10^2$	6·45	6·11	5·40	5·58	5·75	5·25	5·92
	◇	○	○	●	■	◆	◆
	Rough					Transitional	

height y. The drag force on the fence was calculated by integration of the pressure-difference profile and from it, by using (2.6), (2.2) and (2.7), the values of C_{D0} and C_0^* were obtained. A typical pressure-difference profile in dimensionless form is shown in figure 12. The shape of this profile differs from that for a fence in uniform flow (not shown here) at $y/h = 0{\cdot}6$–$0{\cdot}7$ owing to the separation of the boundary layer upstream of the fence in case of boundary-layer flow.

6.4. *Form-drag coefficient of the fence*

Ranga Raju & Garde (1970) showed that a unique relation exists between the form-drag coefficient C_{D0} and δ/h in the case of a smooth wall. This is not so if the wall is rough, with its consequent influence on the velocity profile, as is shown by figure 13. In this figure the data for rough and transitional boundaries are seen to fall below the mean curve for fences on smooth boundaries. Thus, for rough walls constancy of δ/h would be an inadequate criterion for modelling atmospheric flow past structures.

In addition, a plot of the parameter C_0^* *vs.* the parameter h/y' was prepared in accordance with (4.5); see figure 14. In it the data collected during this study as well as the data of Good & Joubert (1968) were used. The data of Plate (1964) and Ranga Raju & Garde (1970) are not included, since the undisturbed boundary-layer profiles of these studies were not detailed enough to enable computations of u_*. Figure 14 shows clearly that C_0^* is uniquely related to h/y' for all flow regimes. The parameter u_*/U_0 has no influence on the drag coefficient of the fence. This implies in effect that U_0 (which affects only the velocity profile

Fig. A-6